Historic, Archive Document

Do not assume content reflects current scientific knowledge, policies, or practices.

aSB608
.D6W43
Copy 2

24

REMOTE SENSING APPLICATIONS IN FORESTRY

THE DEVELOPMENT OF SPECTRO-SIGNATURE INDICATORS OF ROOT DISEASE IMPACTS ON FOREST STANDS

by

F. P. Weber
J. F. Wear

Pacific Southwest Forest and Range Experiment Station
Forest Service, U. S. Department of Agriculture

Annual Progress Report 30 September, 1970

A report of research performed under the auspices of the

Forestry Remote Sensing Laboratory,
School of Forestry and Conservation
University of California
Berkeley, California

A Coordination Task Carried Out in Cooperation with
The Forest Service, U.S. Department of Agriculture

For

EARTH RESOURCES SURVEY PROGRAM
OFFICE OF SPACE SCIENCES AND APPLICATIONS
NATIONAL AERONAUTICS AND SPACE ADMINISTRATION

NR-06-00644

AD-33 Bookplate
(1-48)

NATIONAL

AGRICULTURAL

LIBRARY

aSB608
.D6W43
Copy 2

REMOTE SENSING APPLICATIONS IN FORESTRY

THE DEVELOPMENT OF SPECTRO-SIGNATURE INDICATORS OF ROOT DISEASE IMPACTS ON FOREST STANDS

by

F. P. Weber
J. F. Wear

Pacific Southwest Forest and Range Experiment Station
Forest Service, U. S. Department of Agriculture

Annual Progress Report 30 September, 1970

A report of research performed under the auspices of the

Forestry Remote Sensing Laboratory,
School of Forestry and Conservation
University of California
Berkeley, California
A Coordination Task Carried Out in Cooperation with
The Forest Service, U.S. Department of Agriculture

U. S. DEPT. OF AGRICULTURE
NATIONAL AGRICULTURAL LIBRARY
SEP 22 1986
CATALOGING = PREP.

For

EARTH RESOURCES SURVEY PROGRAM
OFFICE OF SPACE SCIENCES AND APPLICATIONS
NATIONAL AERONAUTICS AND SPACE ADMINISTRATION

Rec'd 7-16-71 2c.

409489

Frontispiece--A view looking east from the center of the Wind River study area. Photograph was taken from the top of the westernmost tower and shows the tramway system which carried radiation sensors over the tops of the study trees. Note the electrical cabling trailing the tramcart in the background which carries sensor signals to the data logger located in the mobile laboratory.

ABSTRACT

The apparent failure in the past of color and color infrared photography to reveal the location of incipient Poria weirii root rot centers in Douglas fir prompted us to consider other remote sensing media. Some preliminary information on apparent temperatures of individual infected trees suggested that thermal infrared might be useful.

In summer 1969 we began a field research program, intensified in 1970, on the physiology and biophysical responses of second growth Douglas fir infected with root rot fungus. A double tramway system was suspended between three 100-foot instrument towers to carry sensors for measuring the energy response from above both healthy and infected trees (Frontispiece).

We found little in the thermal infrared data to suggest that there might be radiant exitance differences between tree condition classes. In fact, from intensive analysis of four months of data, only isolated examples of thermal differences were found between healthy and infected trees. Those anomalous cases could not be related to any physiological or environmental phenomenon.

Processing and analysis was completed of airborne multispectral scanner imagery collected by The University of Michigan over the Wind River research area in 1969. Intensive examination of airborne thermal infrared data by both analog and digital processing did not reveal thermal radiance differences which were related to root rot infection.

Likelihood ratio processing of 3-channel infrared data and Euclidean distance analysis of 10-channel spectrometer data, both processed on SPARC at Willow Run Laboratories, did not identify incipient root rot infection outside the training sets. In all cases infected fir was misclassified as

healthy fir. Both SPARC processes produced excellent recognition maps of forest type and tree species and easily discriminated forest type from nonforest type.

We concluded from careful examination of physiological data that Poria root rot infection has little effect on water metabolism and energy exchange. What was identified was more of a low-grade stress that affects respiration and metabolism over long periods of time. This we surmise led to minor changes in the external physical symptoms of Poria-infected trees which was revealed only in the shortwave reflectance data. That is, the infected trees consistently had a two percent higher albedo at midday. Together with our airborne multispectral data this finding suggests that if incipient infection centers are to be detected by remote sensing in the future, it will be with improved registered sensors operating in the range between .32 and 2.6μm.

A significant discovery in the aerial detection of Poria weirii infection centers in Douglas fir was the identification of root rot signature indicators on 1:15,840 scale panchromatic photography. The recognition feature was large openings or holes in the forest canopy that have an unusual ringworm like appearance. This finding contrasts with research which has attempted to identify small incipient infection centers by thermal symptoms of root rot stress in Douglas fir trees. A preliminary field examination of several of the circular openings clearly identified Poria weirii as the primary agent causing Douglas fir and hemlock mortality. This new signature indicator is a most promising step forward in locating large, well established root rot infection centers in the high Cascades of Oregon and Washington.

ACKNOWLEDGEMENTS

This research was performed under the Earth Resources Survey Program in Agriculture/Forestry under the sponsorship and financial assistance of the National Aeronautics and Space Administration, Contract No. R-09-038-002.

The cooperation and assistance of the following organizations is gratefully acknowledged:

Bonneville Power Administration, U.S. Department of Interior, Vancouver, Washington.

NASA-USDA Forestry Remote Sensing Laboratory, University of California, Berkeley, California.

Pacific Northwest Forest and Range Experiment Station, U.S. Forest Service, Portland, Oregon.

Pacific Northwest Regional Office, U.S. Forest Service, Portland, Oregon.

Pacific Southwest Forest and Range Experiment Station, U.S. Forest Service, Berkeley, California.

Stanford University, Department of Geology, Palo Alto, California, Dr. Ron Lyon.

Wind River Nursery, Gifford Pinchot National Forest, U.S. Forest Service, Carson, Washington.

Special thanks are extended to Mr. Forrest Deffenbacher, Superintendent of the Wind River Nursery, and Mr. David Jay, Ranger of the Wind River Forest District, and to all their personnel for their continuing support of providing storage and shop facilities, vehicles, special equipment, and manpower.

We would like to acknowledge the photographic contribution of Wally Guy and the outstanding photo laboratory work of Richard Myhre of the PSW Remote Sensing Project.

The time and experience of many technical and professional scientists were willingly contributed to the development of sound techniques and methods

to expand knowledge of the root rot disease problem that so vitally affects one of our major natural resources. One such individual, Mr. Philip Collier of the Bonneville Power Administration, provided considerable assistance with his instrumentation know-how.

Special thanks are extended to Mrs. Joyce Dye and Miss Marilyn Wilkes, two of our computer programmers working at the Pacific Southwest Forest and Range Experiment Station in Berkeley, California. It is difficult to measure their contributions because they not only wrote the computer tape handling and analysis programs but continued to update the programs so that current data were always available.

We would like to acknowledge the substantial contributions of Mrs. Anne Weber, Miss Margaret Dugan and Miss Mary Twito, who did our bookkeeping and report typing.

Finally, the responsibility of supervising the field research data gathering and keeping the equipment going was assigned to Mr. James Von Mosch. He, more than any other single individual, is praised for his initiative and conscientious efforts in keeping the research program viable.

TABLE OF CONTENTS

Frontispiece i

Abstract ii

Acknowledgements iv

Introduction 1

Instrumentation and Methodology 4

Biophysical and Physiological 4

Radiation Sensors 5

Physiology Sensors 6

Environmental Sensors 7

Data Logger 9

Airborne 10

Cameras 10

Optical-Mechanical Scanners 11

Multispectral Processing of 1969 Imagery 13

SPARC 13

Thermal Analog 15

Digital 16

Results 17

Biophysical and Physiological Evaluation 17

Photographic Evaluation 31

Multispectral Evaluation 32

Summary 39

Remote Sensing Rationale 39

Biophysical and Physiological Implications 40

Multispectral Imagery 41

Future Research 42

Literature Cited 45

Appendix 46

THE DEVELOPMENT OF SPECTRO-SIGNATURE INDICATORS OF ROOT DISEASE IMPACTS ON FOREST STANDS

F. P. Weber and J. F. Wear

Pacific Southwest Forest and Range Experiment Station
Forest Service, U. S. Department of Agriculture
Berkeley, California

INTRODUCTION

Multispectral remote sensing research continued to provide information in 1970 on forest disease problems that continually create a severe impact on our nation's forest resource. Diseases are of great concern to all forest owners and land managers because of the millions of board feet of valuable timber destroyed or degraded each year. Approximately 170 million board feet of timber in the United States are destroyed each year by the root rot disease, Poria weirii (Murr.). Heaviest losses from this disease occur in extensive stands of Douglas fir (Pseudostuga menziesii (Mirb) Franco), a major commercial timber species of the Pacific Northwest.

This is the sixth annual report on continuing research to discover remote sensing techniques for aerial identification and impact evaluation of Poria weirii infection centers. For the last two years our principal research effort has been the biophysical and physiological assessment of trees under stress from root rotting fungus as compared to healthy trees.

Results in 1967 and 1968 of airborne thermal infrared data recorded with a Barnes PRT-5 radiometer indicated significantly higher apparent temperatures of Poria-infected trees. Tests were flown in a helicopter at 150 feet above the tree crowns of young growth, second growth, and old growth

Douglas fir stands in Washington. Flights were made in spring, summer, and fall at three times during the day. However, results varied from time to time, indicating the need for more precise ground truth.

Although a great deal of work was done on aerial instrumentation during the initial stages of the research program prior to 1969, little was really known about the relationship between root infection and the expression of stress through the impairment of physiological processes. We felt a greater understanding was needed of the biophysical and physiological implications of stress to airborne remote sensing.

In 1969 we constructed a three-tower, double aerial tramway system for placing energy sensors over the tops of our research trees, both healthy and root rot infected. The details of the construction and initial operation of the aerial tram system are discussed in our 1969 Annual Report.

A major improvement in the efficiency of our field research program this year was provided by the addition of a Vidar 5403 digital data logger (Figure 1). This system permitted precise sensor recording in the microvolt range at a maximum rate of 35 channels per second.

Multispectral data collected by the University of Michigan airborne optical-mechanical line scanner system in July and September, 1969, over our Wind River research area have been processed and analyzed. The results were not encouraging in terms of aerial thermal detection of Poria infection centers but were well correlated with our ground data.

The recent discovery of Poria weirii infection centers on 1:15,840 scale panchromatic photography, with verification by field inspection, signals the change in emphasis of our research from previsual and thermal approaches back to aerial photography. Emphasis for the future will be directed toward this promising and practical signature indicator which is identi-

Figure 1. A Vidar 5403 data acquisition system was used to digitize biophysical and physiological sensor data and record it onto magnetic tape for computer analysis. Data logger was operated in two different modes: (1) scanning all 38 sensors once each 20 minutes while the tramways were parked over benchmark trees, and (2) scanning continuously at one channel per second while the tramways were moving.

fied by an unusual ringworm-like appearance on small-scale photography.

INSTRUMENTATION AND METHODOLOGY

Research data gathering at Wind River was keyed to sampling benchmark study trees (three healthy and three root rot infected) which were located directly beneath the double tramway system (Frontispiece). The two tramways each carried longwave and shortwave energy sensors and were programmed to operate in two different modes: (1) sampling energy data every 20 minutes while parked over one healthy and one diseased tree, and (2) sampling data continuously while both of the trams were moving. Data were gathered for more than 120 continuous days and nights beginning in mid-May. From the physiological standpoint, the experimental period extended throughout one complete soil-water cycle, from field capacity through summer drought and into the beginning of the rainy season.

Biophysical and Physiological Instrumentation

Sensors were placed in contact with or in proximity to study trees depending on the parameter being measured. Almost all measurement techniques employed some sort of electromechanical sensor which sent a voltage signal via transmission lines to the data logger. The principal purpose of ground sampling was to establish energy and water balance relationships between healthy and stressed trees as functions of variations in environment due to time of day or season.

Radiation Sensors

Incident radiation. A Kahl Scientific Star pyranometer was used to measure incident shortwave radiation. The Star was normally oriented and positioned on top of the center 33-meter tower and measured incoming hemispher-

ical shortwave radiation. Our pyranometer had been tested beside an Epply pyranometer, which is generally accepted as a standard instrument for incident radiation measurement. No difference was determined between the measurements of the two instruments.

Reflected radiation. Two inverted Star pyranometers were used to measure reflected shortwave radiation above the forest canopy. One sensor traveled on a tramway over healthy trees, and the second was carried over the diseased trees. Reflected energy, computed as a ratio with incident energy, was used to calculate albedo. These values were computed only during daylight hours.

Net allwave radiation. A pair of Kahl Scientific net allwave radiometers was mounted on each tramway, one to provide primary data and the second as a standby backup. A problem developed at one point during the summer which required the use of data from the backup net radiometer. The electrical lead for the primary net radiometer became fouled in the tramway pulleys and separated. In contrast to 1969, when we were developing the techniques for the tramway operation, this was the only occurrence of data interruption resulting from tramway problems.

Radiant exitance. A radiometric device was designed for incorporation in the net radiometers which measured radiant exitance within the field of view of the sensor. These data provided a precision measurement of emitted energy of individual trees, which was comparable to that sensed by the 8 to 14 μm detector of Michigan's airborne optical-mechanical scanner system. As near as could be determined, about 95 percent of the energy sensed by the radiometric plate came from within a three-degree field of view. This meant that because of the height of the plate above the trees, multiple samples could be attained wholly within the crown of an individual tree. The ad-

vantage of this device was that it was known to always have a fixed vertical focal point which was useful for determining the effect of sun angle on radiant exitance measurements.

Physiology Sensors

Sap flow. Improvements were made this year in the system for measuring the rate of upward translocation of water in the study trees. Two detectors were installed on opposite sides of the tree boles of two healthy and two root rot infected trees. Heat pulse data, indicating the rate of water movement, were transmitted back to the master control recording device located in the mobile laboratory. Data from the eight sample points (taken one and one-half meters above the root collar) were recorded simultaneously 18 times every 24 hours.

Xylem sap pressure. Once each week during the summer, small branch samples were taken from six sampling points in the upper crown of each study tree. As the branch samples were dropped to the ground, they were taken into the laboratory and inserted into a hydrostatic pressure chamber to measure xylem sap pressure. Related studies with ponderosa pine had shown a strong relation between rate of sap flow, xylem sap pressure, and tree vigor. Sap pressure was identified as the best physiological indicator of tree stress and vigor decline as related to aerial remote sensing (Weber, 1969).

Leaf temperature. Micro thermocouples of copper-constantan were used to measure leaf temperature. Although it required a large investment of time for initial installation, we felt it was worthwhile in the event the radiometric plates did not function as designed. Thermocouple compensation and linearization were accomplished with an Acromag model 350 double-oven reference device. The Acromag compensator operated day and night throughout the

summer with no failures.

Wood defect. A new approach was applied this summer to the evaluation of root rot presence in living trees. We tested an acoustical sensor which measures wood defect. In the past, determination of infected trees was accomplished by extracting increment cores from the center of the tree near the base. The presence or absence of Poria weirii was determined by indication of punky wood (advanced state of rot) or brown-stained wood (incipient to moderate stages of fungus spread).

In an attempt to improve the time-consuming traditional method of root rot identification on the ground, we tested a Pol-tek acoustical sensor (Figure 2) belonging to the Bonneville Power Administration. This acoustical sensor had been useful to their field crews for identifying decay and defects in standing power and telephone poles. It was shown to detect rot, voids, and airpockets in dry wood with differential sound waves traveling through a test pole between a sending and receiving probe. Test readings were made on two different sides of a tree. Actual rot evaluation was ascertained from increment core samples.

Environmental Sensors

Rainfall. Rainfall was measured at an ESSA weather station established near the Wind River Ranger Station. Inasmuch as the personnel there used a standard rain gauge and collected the rainfall data in a prescribed manner, there seemed little point in establishing another monitoring station in such close proximity. The data we needed were readily available to us through the Ranger.

Soil moisture. Soil water content was monitored once each week with a neutron density probe. The radium-berrylium source was contained in a Nuclear-

Figure 2. Acoustical sensor used to determine decay in power and telephone poles may be effective in determining presence of rot in living trees. The two probes shown are held on opposite sides of the bole, a sound wave is transmitted, and the time interval to pass through the diameter of the log is recorded on the lightweight, transistorized instrument.

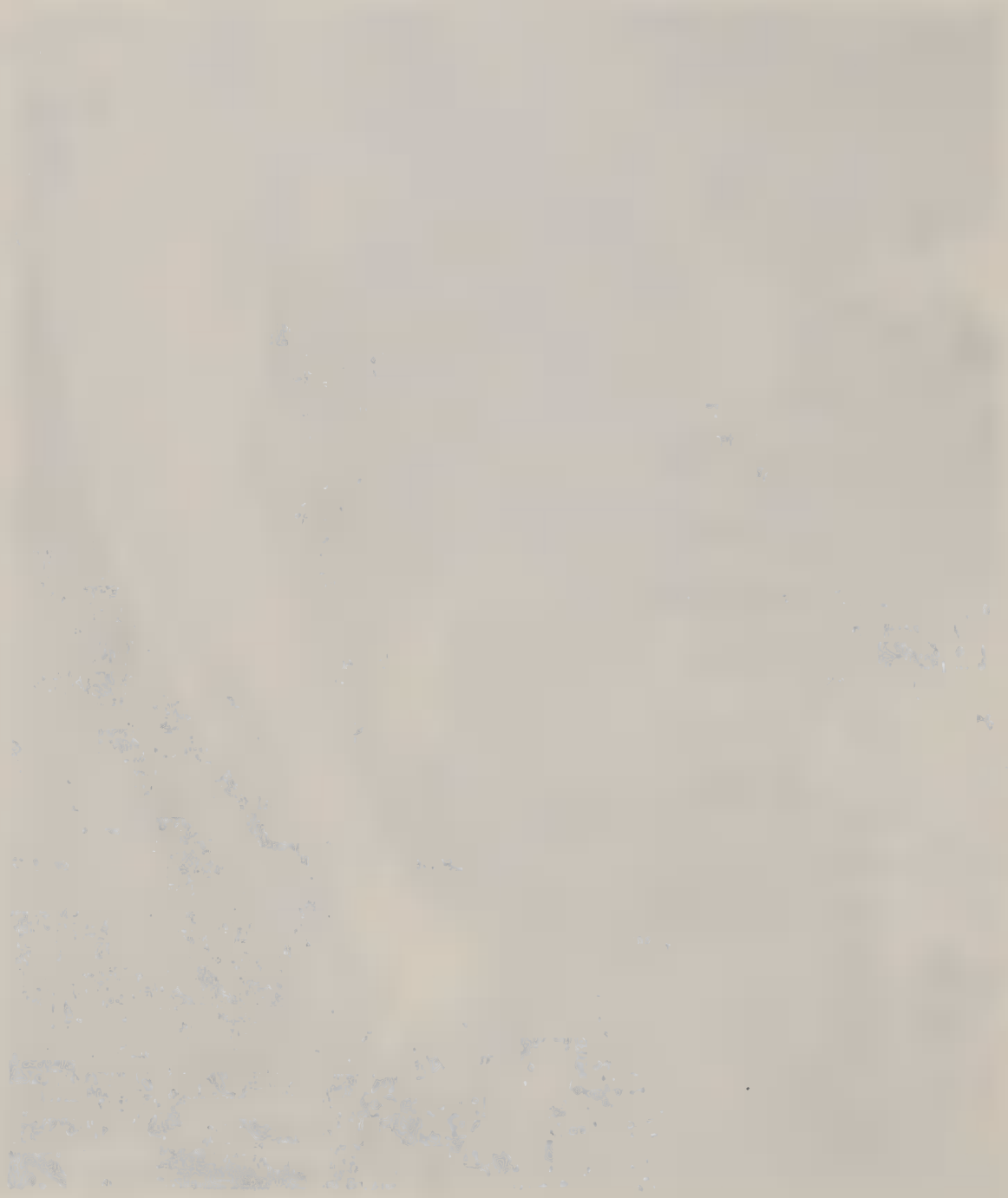

Chicago P-19S soil moisture probe which, together with the counter, had been thoroughly reconditioned and tested before the field season. Soil water profiles were measured in 16 access tubes surrounding healthy and infected trees.

Wind speed. The flow of wind currents is quite predictable at Wind River in the summer, both in terms of direction and intensity. Even so, we used one anemometer placed atop the westernmost tower to monitor wind movement. Wind data were transmitted to a translator in the mobile laboratory and were then recorded on the data logger. The anemometer was sampled by three separate channels on the data logger so as to develop a reliable average wind speed for each sample period.

Dew point. Atkins Scientific dew point sensors were used to record dew point information needed to calculate vapor pressure deficit and relative humidity. Although the Atkins sensors and translator are relatively inexpensive, they are accurate, have a quick response time, and functioned without service day and night throughout the summer. Dew point sensors were located as follows: (1) in the mid-crown of a healthy tree, (2) in the mid-crown of a diseased tree, and (3) inside a standard weather shelter two meters above the forest floor.

Ambient air temperature. Air temperature was measured with shielded copper-constantan thermocouples at five locations throughout the study area distributed from ground level to the top of the general crown canopy.

Data Logger

The Vidar 5403 digital data logger was specifically designed and engineered for data collection and control functions in our research study. Our original plan had been to purchase a system that included a small operational computer to perform control functions as well as convert data to engineering

units for display in real time. The higher than expected cost did not permit inclusion of the computer portion, but the rest of the data logger was not compromised.

Data were collected for about ten days at a time on digital magnetic tape, after which the tapes were sent directly to our computer facility in Berkeley. Raw data were identified as to recording mode, converted to engineering units, reformated, and rewritten onto two separate tapes (one for each data mode) for computer analysis. A second step was to analyze the data from each of the new data tapes and to print out the results, hour by hour and day by day.

The Vidar system operated continuously for $2\frac{1}{2}$ months faultlessly until an integrated circuit went bad in the scanner and caused some problems during the remainder of the summer. Being located in a remote area 800 miles from the Vidar plant caused some understandable delay with identification and correction of the problem. However, the manufacturer provided a unit on loan which provided continuity in data collection with less than one day of lost time.

Airborne Instrumentation

All airborne data collection reported here was performed by the University of Michigan multispectral system during summer 1969. It is being reported at this time as analyses of the fully processed data were just completed. Airborne flights occurred on July 14 and 15, 1969, and on September 26, 1969.

Cameras

Four J. A. Maurer P-220 70 mm. aerial cameras recorded photographic data from the Michigan aircraft. Each camera was fitted with a 75 mm. lens and operated at the maximum shutter speed permitted by the combination of

optical aperture and film emulsion speed. The cameras employed the following film/filter combinations: (1) Aerial Plus-X panchromatic film with a Wratten 25A (red) filter; (2) Aerographic infrared film (B/W) with a Wratten 25A (red) filter; (3) Ektachrome film with a Wratten 1A (haze) filter; and (4) Ektachrome infrared film with a Wratten 12 (minus blue) filter. Due to flight restrictions from the high surrounding terrain, the aircraft was flown 650 meters above the research area with a resulting photo scale of about 1:8,000.

Optical-Mechanical Scanners

The Michigan Multispectral Scanner System flown on this study consisted of two separate double-ended optical-mechanical scanners (Figure 3). The unique feature of the Michigan system was the addition of a prototype spectrometer to end A of the first scanner. The spectrometer collected energy in a fiber optics bundle and provided automatic registration in both time and position for ten discrete spectral bands between .4 and 1.0 μm. End B of the first scanner was fitted with a three-element detector sensitive in the bands 1.0 - 1.4 μm, 1.5 - 1.8 μm, and 2.0 - 2.6 μm. End A of the second scanner was fitted with a narrow field of view (37 degrees) three-element detector sensitive in the bands 1.0 - 1.4 μm, 2.0 - 2.6 μm, and 4.5 - 5.5 μm. End B of the second scanner had a cooled Hg:Ge detector sensitive in the range 8.2 - 13.5 μm. The second scanner was calibrated and recorded direct beam sky radiance; it contained two tungsten filaments, reference plates, and a zero reflectance body on the inside of the scanner.

Scanner data were recorded in analog form on one 14-track tape recorder and one 7-track recorder. Simultaneous calibration and referencing provided rapid access to the data back in the laboratory. Radio communication between the system operator and the field laboratory provided minute by minute ground data for setting airborne system reference levels.

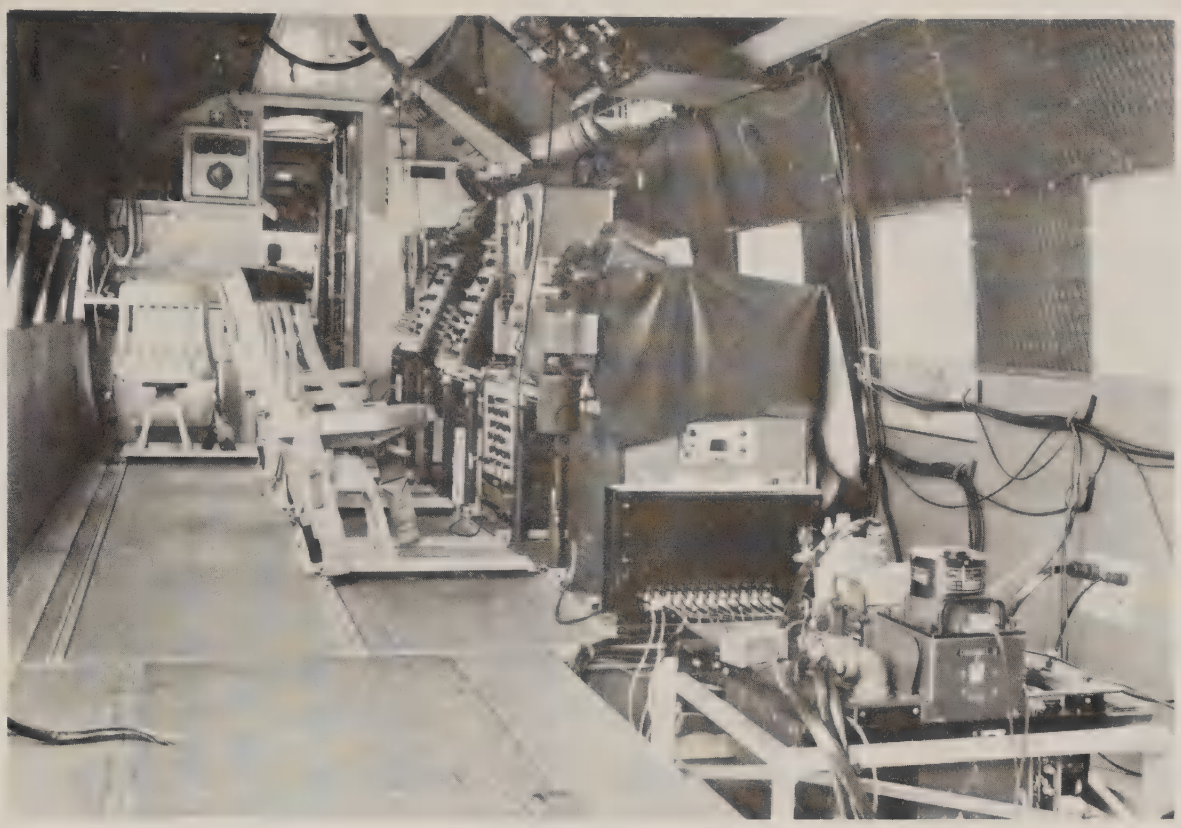

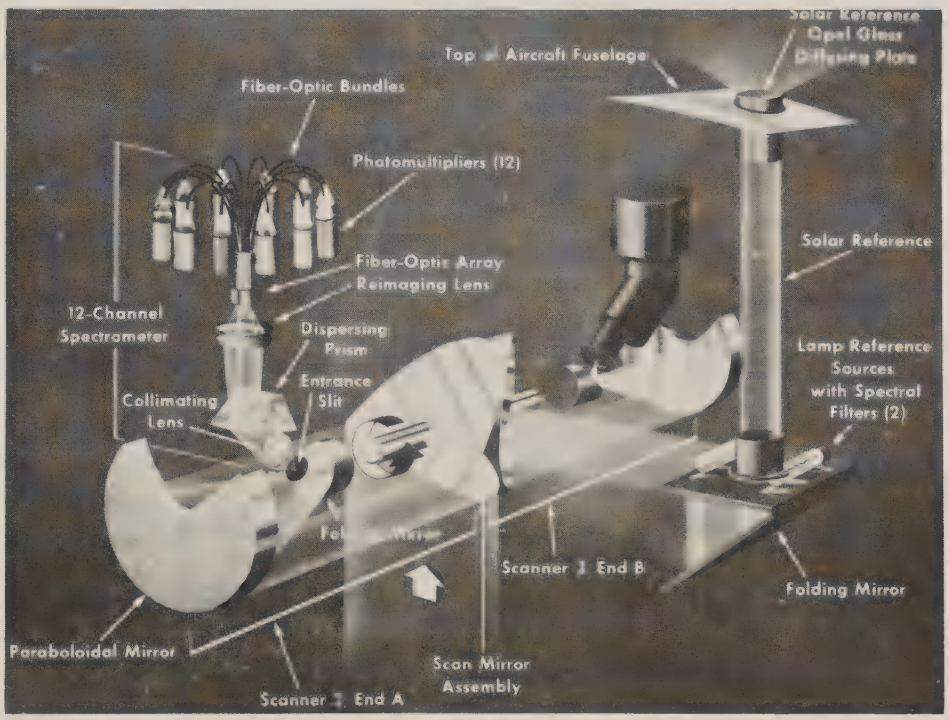

Figure 3. Photograph above shows the interior view of the Michigan multispectral aircraft with the recording and control consoles forward and the multispectral scanners right foreground. Photograph below shows a line drawing of one of the two optical-mechanical scanners. The 12-channel spectrometer is focused on end A and the three-channel IR detector is focused on end B.

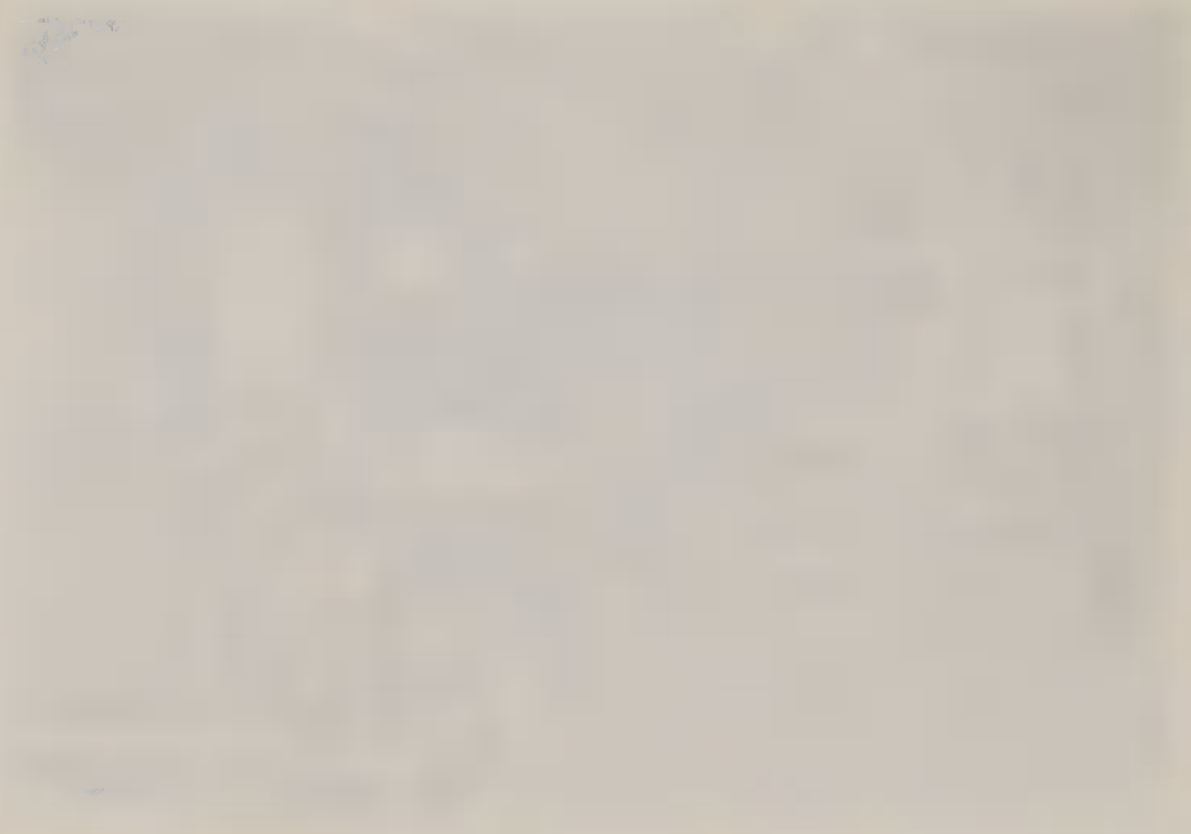

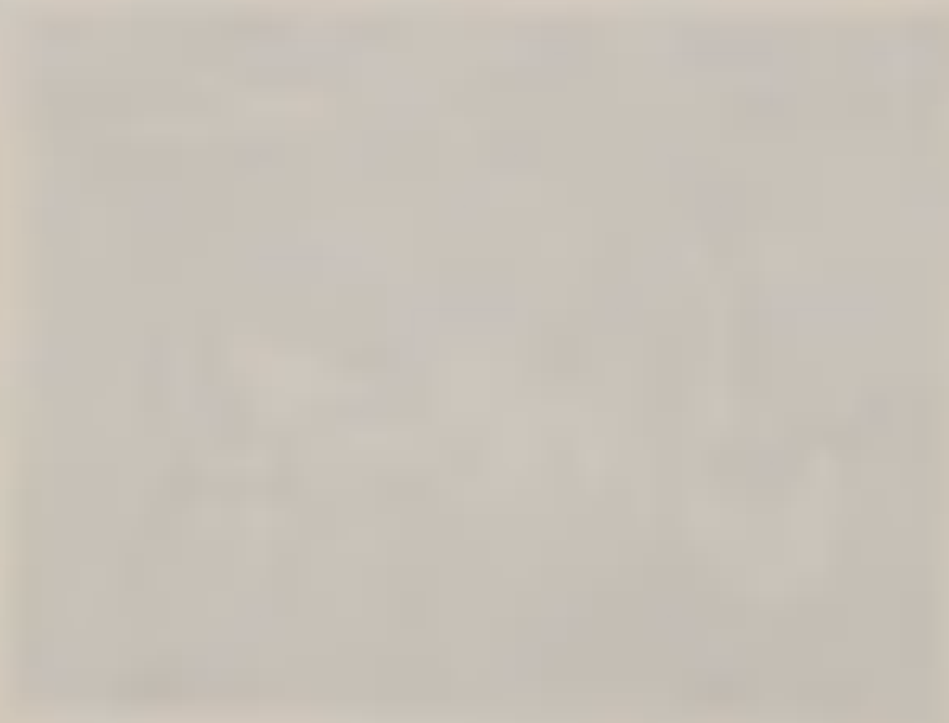

Airborne flights were conducted as follows: (1) within two hours after sunrise, (2) mid-morning, (3) midday, and (4) mid-afternoon. The flight line was about 700 meters long over the research area. Because of the short distance, several runs were flown during each flight to insure sufficient data for at least one run per flight.

Multispectral Processing

All processing of multispectral data was completed at the University of Michigan's Willow Run Laboratories under a master contract, NAS 9-9734, for data processing monitored by NASA Manned Spacecraft Center, TF8.

By November 1969, all aircraft tapes had been duplicated and the preliminary viewing of all video data was completed. At that time, the best runs were selected for intensive processing and analysis, and plans for data processing were worked out with Michigan and our NASA Technical Monitor.

Because the data from several channels were recorded in registration and were referenced, a number of analog and digital processing techniques were available for processing the data.

SPARC Processing

Processing experiments were conducted at Willow Run Laboratories with a special Spectral Processing and Recognition Computer (SPARC--Figure 4). Two separate operations were performed on the SPARC. The first consisted of selecting a training sample from the data (that is, some known point or area in the test scene) and storing the spectral characteristics of that area in the computer. Training sets were selected to describe the total forest scene at Wind River as nearly as possible. They were: (1) healthy Douglas fir, (2) Poria-infected fir, (3) red alder, (4) conifer sub-canopy, (5) hardwood sub-canopy, and (6) forest nursery. The next operation consisted of

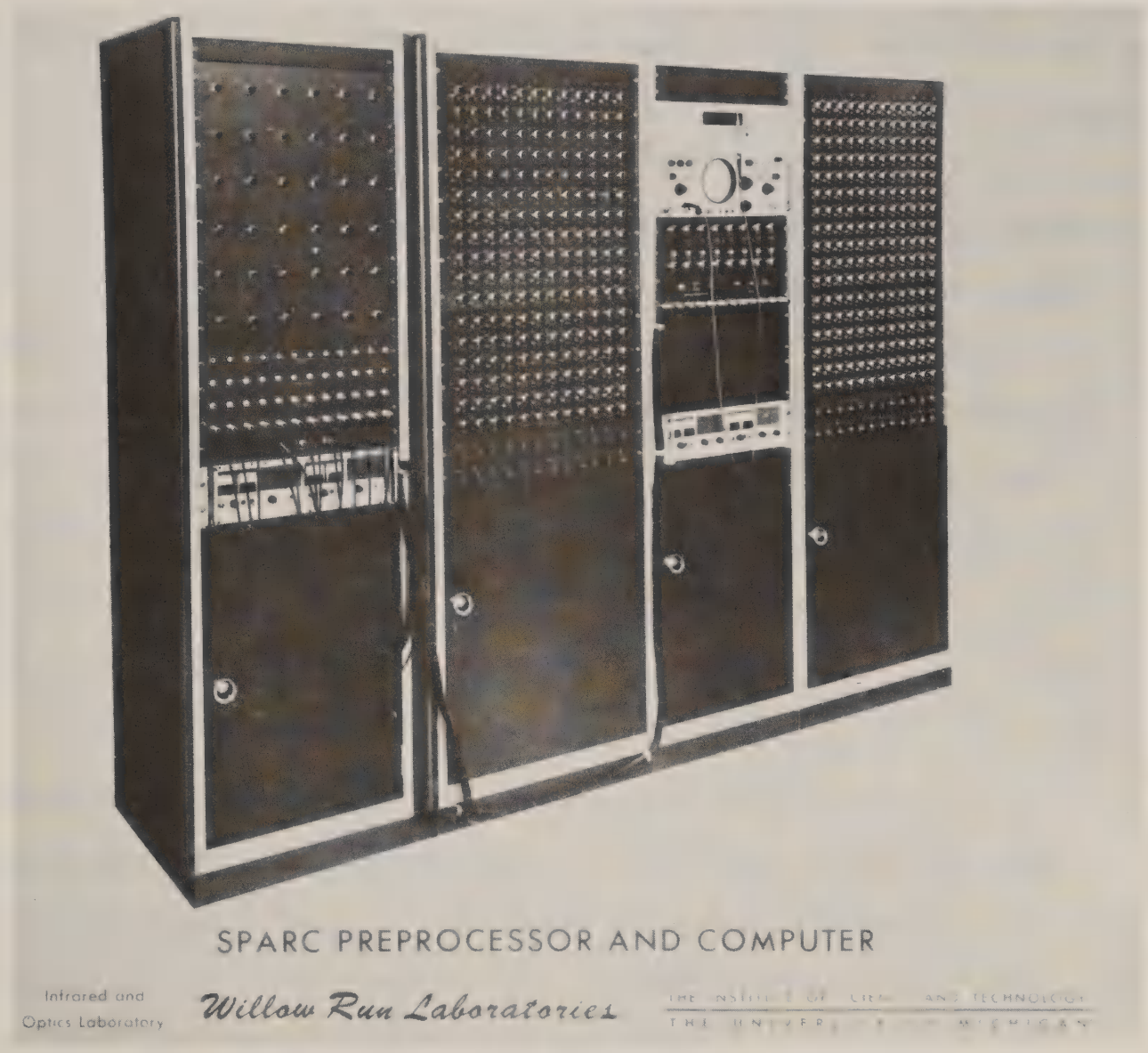

Figure 4. The University of Michigan's special Spectral Processing and Recognition Computer (SPARC) is shown at the right alongside the analog preprocessor. A high quality tape loop playback unit, CRT display, and photo printer are components of the processor not shown.

recognizing all points in the scene which were statistically similar, within predefined criteria, to the spectrum from the training set. A strip map was prepared in which all points with similar spectral properties were printed as an enhanced image. (Details of the mathematics for the decision criteria are given in Lowe et al., 1966.)

Through use of a training set for each of the six objects of interest the process was repeated, and each recognition map was coded with a different color to display in one format the distribution of all objects. Since the area of each resolution element was known, an area count of each set of objects was available immediately at the end of each data run. And since the tape could be played back immediately, data were analyzed without any delay on the computer.

Thermal Analog Processing

Specialized single-channel processing was used with the thermal 8 - 14 μm channel data to produce a set of voltage slices corresponding to different temperature intervals (Nalepka, 1970). Since the raw data were originally stored on magnetic tape, the electronic slicing was performed easily and more accurately than if the object were photographed and subsequently scanned with a densitometer over the grey tones of the film.

The technique consists of slicing the thermal data into a number of equal size voltage increments (usually ten), printing the data contained in each of these increments on film, and color-coding each increment to produce a display of signal amplitude in color. By calibrating each voltage increment with respect to the thermal reference plates in the scanner, and assuming a linear variation of signal amplitude with scene object temperature, we obtained a calibration of each step in terms of temperature.

The width of the slicing interval was set by careful examination of the ground truth data at the time of the overflight. The width of the slicing level was usually taken as one-tenth the total voltage spread between the coldest and warmest targets of interest. The actual slicing increment depends largely on the greatness of variation in the object scene temperatures. The slicing levels at which the hot and cold references occurred were recorded for later calibration of steps in terms of temperature.

Digital Processing

The statistical decision criteria for recognition processing (both thermal and nonthermal) were performed with digital techniques. Also, digital preprocessing programs were used to remove unwanted variations in the data due to angle effects, shadows, and possible scanner nonuniform response over the total field of view to increase accuracy of recognition over the entire imaged flight line.

A technique was developed for looking at the response of the thermal (8 - 14 μm) detector in digital form. A computer program was written to convert the analog signals, with calibration data, to a digital format. The thermal data were sampled 3.8 times per resolution element and quantized before being recorded on digital tapes at 200 BPI. Subsequently, the data were converted to 556 BPI and short records to be compatible with our 1108 computer facility in Berkeley.

The Michigan computer facility produced greymap outputs of the digitized thermal data. Every fourth digitized point and every scan line were printed by the greymap routine. Seven character-densities were used to represent radiance variations within the flight line scene. A digitized range was assigned each characterization and the sensitivity of the display technique could be manipulated depending on the size of each range, that is, the den-

The [illegible] sliding interval was set to certain [illegible] of the
pulsed echo [illegible] at the rise or top of pulse. The width of the sliding
level was normally taken to represent the total voltage spread between the
codebar and maximum target at interest. The actual sliding increment be-
comes largely on the preference of operation or the limit range tolerance
the editor level is at which the not are data relevance. Incorrect word rec-
ter [illegible] distribution of areas in terms of codewords.

Digital Processing

The [illegible] ideal for systems for recognition or assessing (Mon-
theory) the nonlinear) work performed with digital techniques. Also, digital
phonograph [illegible] programs were [illegible] to remove known or variations in the data due
to [illegible] effects, [illegible], and possibly [illegible] of recognition errors. Over the
[illegible] trend or [illegible] to increase accuracy of recognition over the analog [illegible]
[illegible] time.

A [illegible] machine was designed for looking at the response of the channel
(B - [illegible] any deviation in digital form. A control [illegible] program was written to com-
vert the [illegible] theory, with set bits on note, to a digital format. The
[illegible] data were sampled 1.6 times per resolution element and quantized
[illegible] range recorded on digital tapes for use BCL. Consequently, the data-
red to [illegible] that these records to be compatible with our [illegible]

[illegible] by a pulsed [illegible] [illegible] of the digitized
[illegible] and every [illegible] was plotted
[illegible] was used to reconstruct
A digitized range was ob-
by of the display technique

sity levels were spread over both a wide and very narrow apparent scene temperature range. Scan samples and scan lines were numbered on the computer greymap and were easily related to a 3X enlargement of the thermal analog filmstrip for point identification.

RESULTS

Biophysical and Physiological Evaluation

Extensive ground instrumentation is frequently needed to establish physiological stress parameters in forest trees and also to provide ground truth for airborne multispectral data. Such was the case with research at Wind River, where we conducted basic studies to answer the fundamental questions about changes in tree physiology and biophysical responses of Poria weirii infected trees in relation to seasonal and diurnal changes in the environment of a Douglas fir forest.

Because of our beliefs regarding the nature of Poria weirii within Douglas fir prior to 1970, we expected to find large differences in water metabolism of affected trees compared to healthy trees. This, we felt, would be the key to understanding leaf temperature and energy exchange differences, if they existed. Rainfall and the availability of water in the soil-root horizon, then, became important variables to measure. The null hypothesis that we tested was that there was no difference in radiant exitance between healthy and rot-infected firs.

In comparison to the average for the past 20 years, rainfall during 1970 (Figure 5) at Wind River was normal. Soil water content was surprisingly high, especially in the soil strata where active roots were prevalent. Normally the soil water content near the surface degrades more significantly when recharge from rainfall is lacking, and soil moisture stress would be

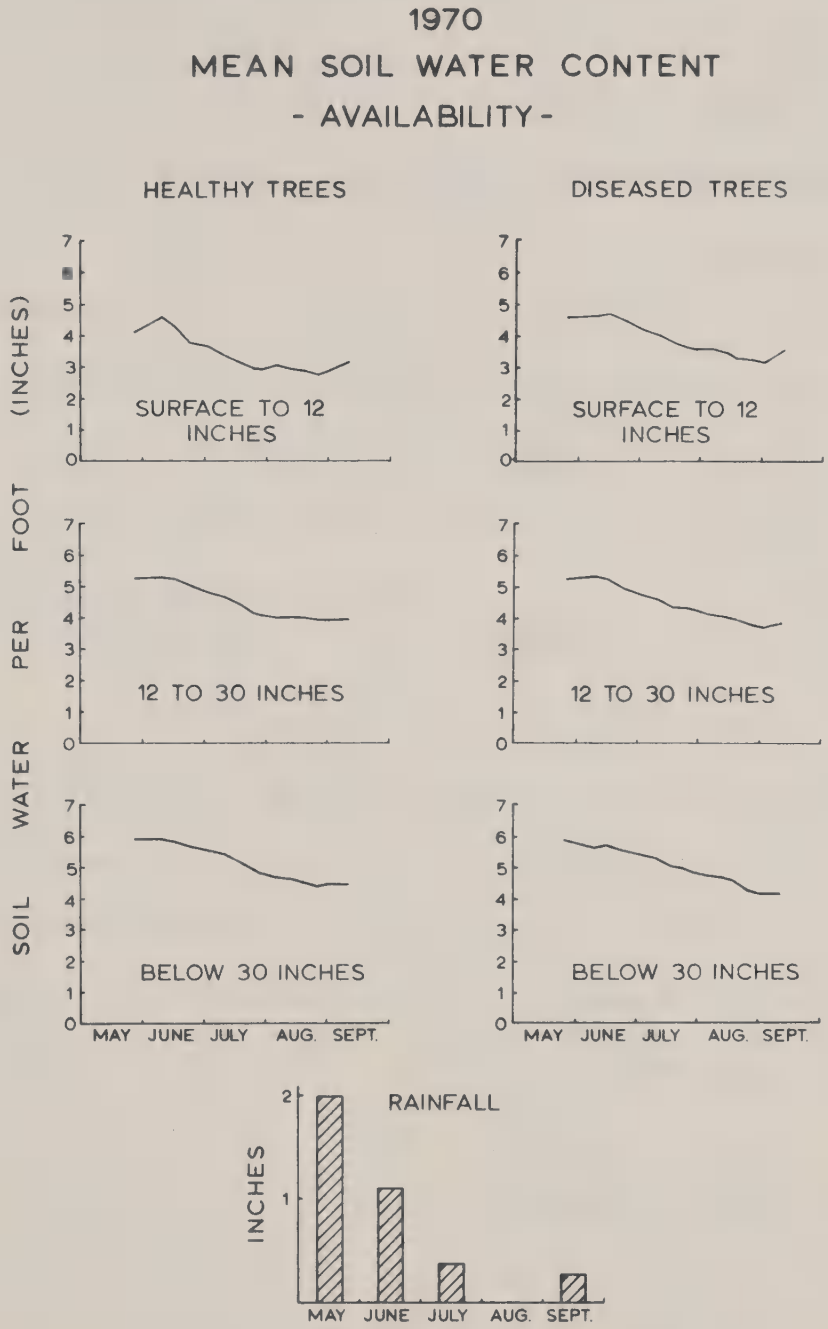

Figure 5. A comparison of mean soil water content at the Wind River research area for 1970, surrounding healthy and Poria weirii infected study trees. Data were calculated from neutron probe soil profile measurements made each week at 16 access tubes. Rainfall at Wind River for the same seasonal period is also given.

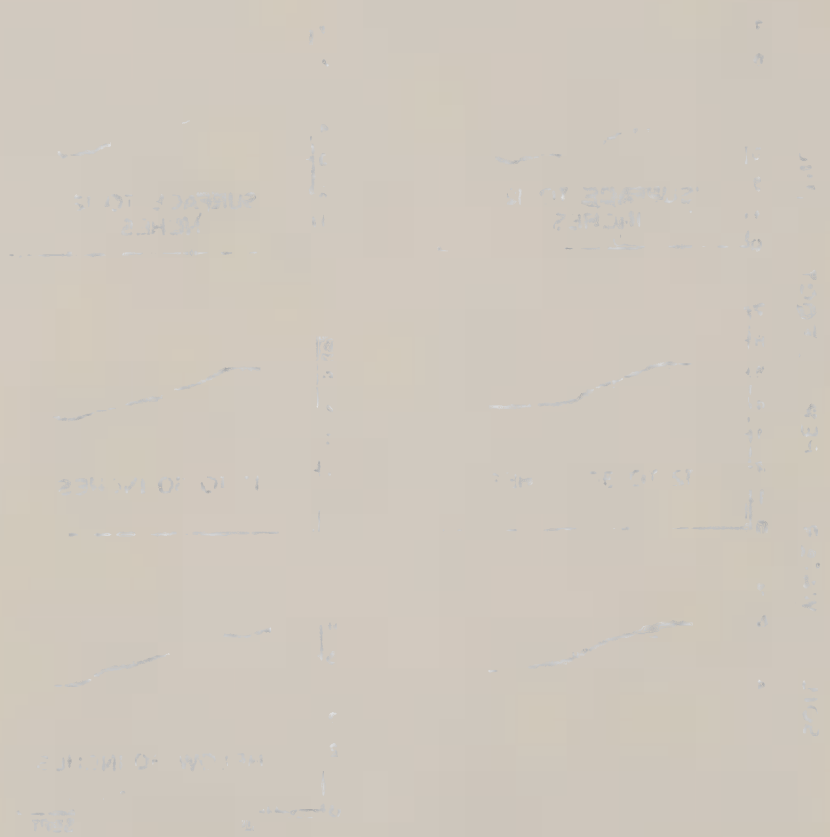

imposed on all trees regardless of other internal manifestations. We discovered that subsurface recharge was provided throughout the summer from a high water table.

Sap flow or the rate of vertical rise of water in conifers is well correlated with both soil moisture availability and xylem sap pressure. That is, in a normal tree, sap velocity is a function of an unbroken hydrostatic gradient between the roots and the mesophyll cells in the leaves. If Poria spread were to have a significant impact on water metabolism it would have to substantially affect the upward flow of water. This disruption should be reflected in reduced sap flow velocity and not just in the physical deterioration of a portion of the root structure.

Our results showed very little reduction in the rate of sap flow of Poria-infected trees. The largest difference was measured during the last week in August (Figure 6). The minor reduction in sap flow at noon for both healthy and diseased trees is a response to midday transpirational lag. If a tree has occluded xylem cells within a normally active translocation zone, the rate of sap flow will characteristically increase late in the afternoon and remain high until late evening. Such was not the case with our diseased trees.

Xylem sap pressure (or leaf moisture tension) can be an excellent parameter for judging the water balance of Douglas fir, especially as it relates to leaf moisture stress. If we were to use this criterion in judging the vigor of trees at Wind River, we would conclude that the healthy study trees were really the individuals under greater stress. Except for two of the weekly sampling periods at Wind River (Figure 7), the average sap pressure values for healthy trees were higher than those for infected trees. The within-tree variations were usually small, indicating a sufficient sample

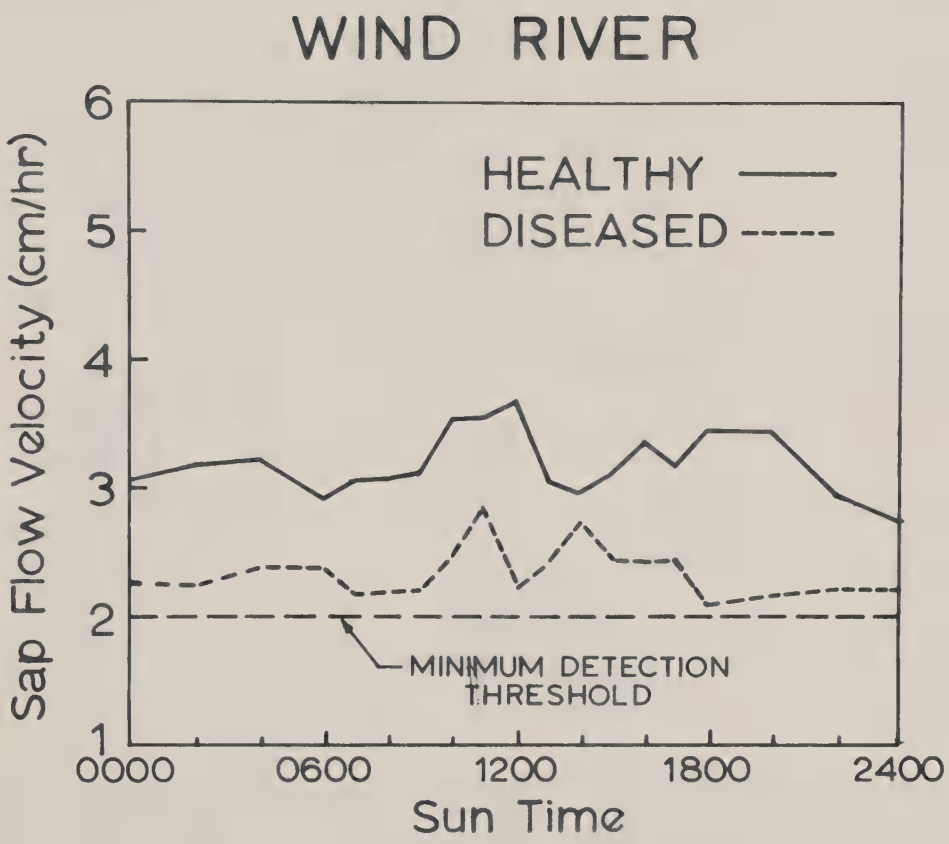

Figure 6. A comparison of vertical sap flow in healthy and Poria weirii infected trees (average hourly rate combined for the last seven days in August, 1970). Input data were provided by sensors on two healthy and two distressed trees. The difference in sap flow shown is the largest such difference measured during the summer. The general level is about 20 percent of the normal springtime sap flow velocity.

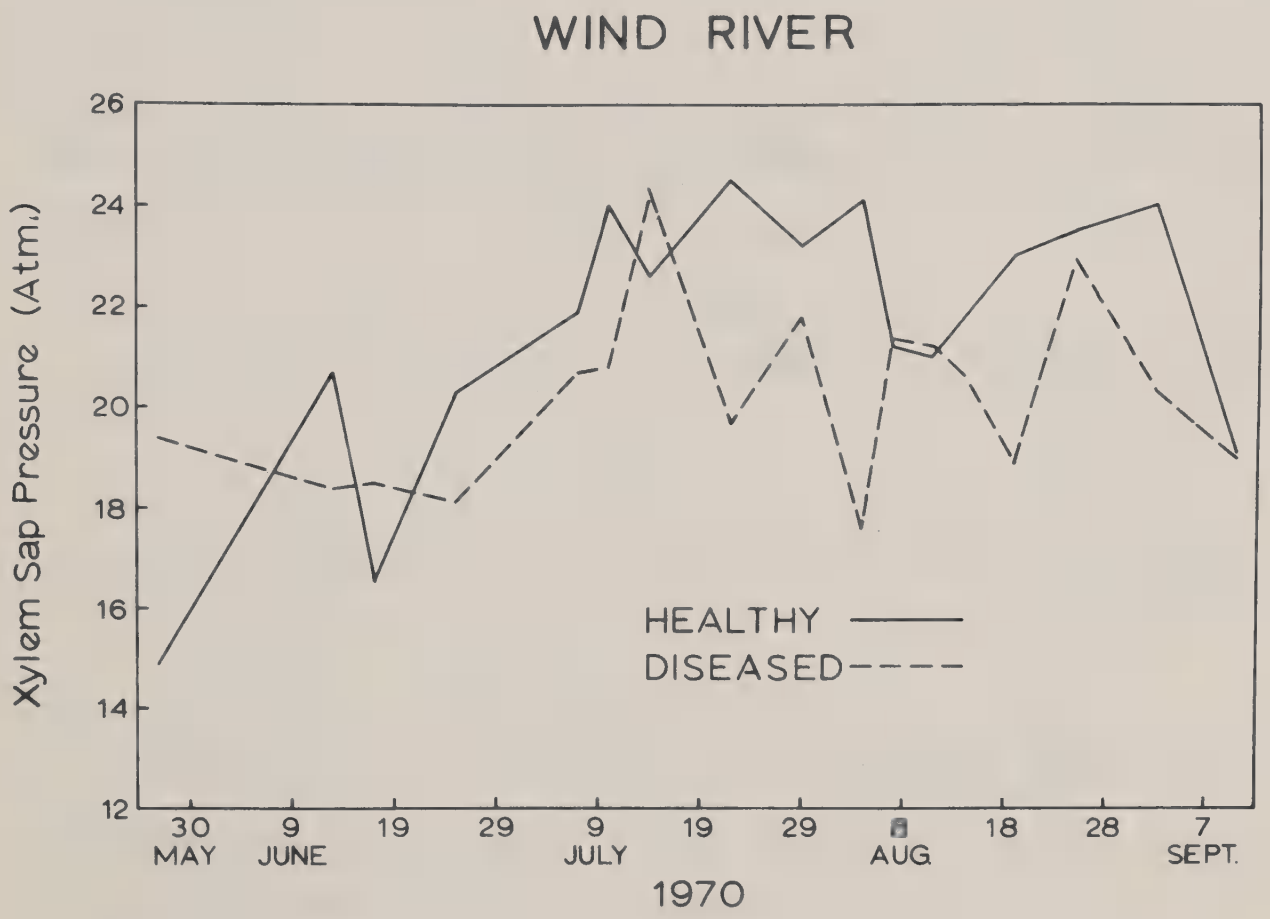

Figure 7. A weekly comparison of xylem sap pressure measurements shows an inconsistent relationship between healthy and diseased Douglas fir. Weekly plotted values are based on measurements of six branch samples from each of seven study trees.

size. Within condition class variations were also small, but more irregular, between diseased trees than between healthy trees. All sample trees were close to the same size and were the same age. Branch samples were taken from the same parts of all tree crowns. The fact that sap pressure samples were always taken early in the morning does not provide a tenable explanation for the variable results because, at that time of day, sap flow velocity readings were usually about the same.

Sample days for looking at the details of energy balance (Figures 8 - 12) were selected at weekly or biweekly intervals based on the existence of cloud-free sky conditions. This was done because on cloudy days no differences were ever measured between healthy and Poria-infected trees.

Energy balance data must be viewed with a clear understanding of their implications to remote sensing; thus, the following explanation:

Solar radiation is a measure of incident shortwave (.4 - 4.0 μm) energy which is largely responsible for the rate of physiological functions at any point in time, as well as determining the potential emission energy for remote sensing.

Albedo is the ratio of reflected shortwave energy to incident shortwave energy. The importance to remote sensing is that albedo provides a measure of expected contrast ratios between objects of interest. It shows which objects may appear brightest on spectrometer imagery, based on reflected energy, within the scene.

Net allwave radiation is important to the interpretation of remote sensing data because it measures directly the allwave (.4 - 15 μm) incident energy minus the allwave reflected and emitted energy. For example, a stressed tree which has a lower value net allwave radiation state than its neighbor will have a higher reflected or emitted energy component.

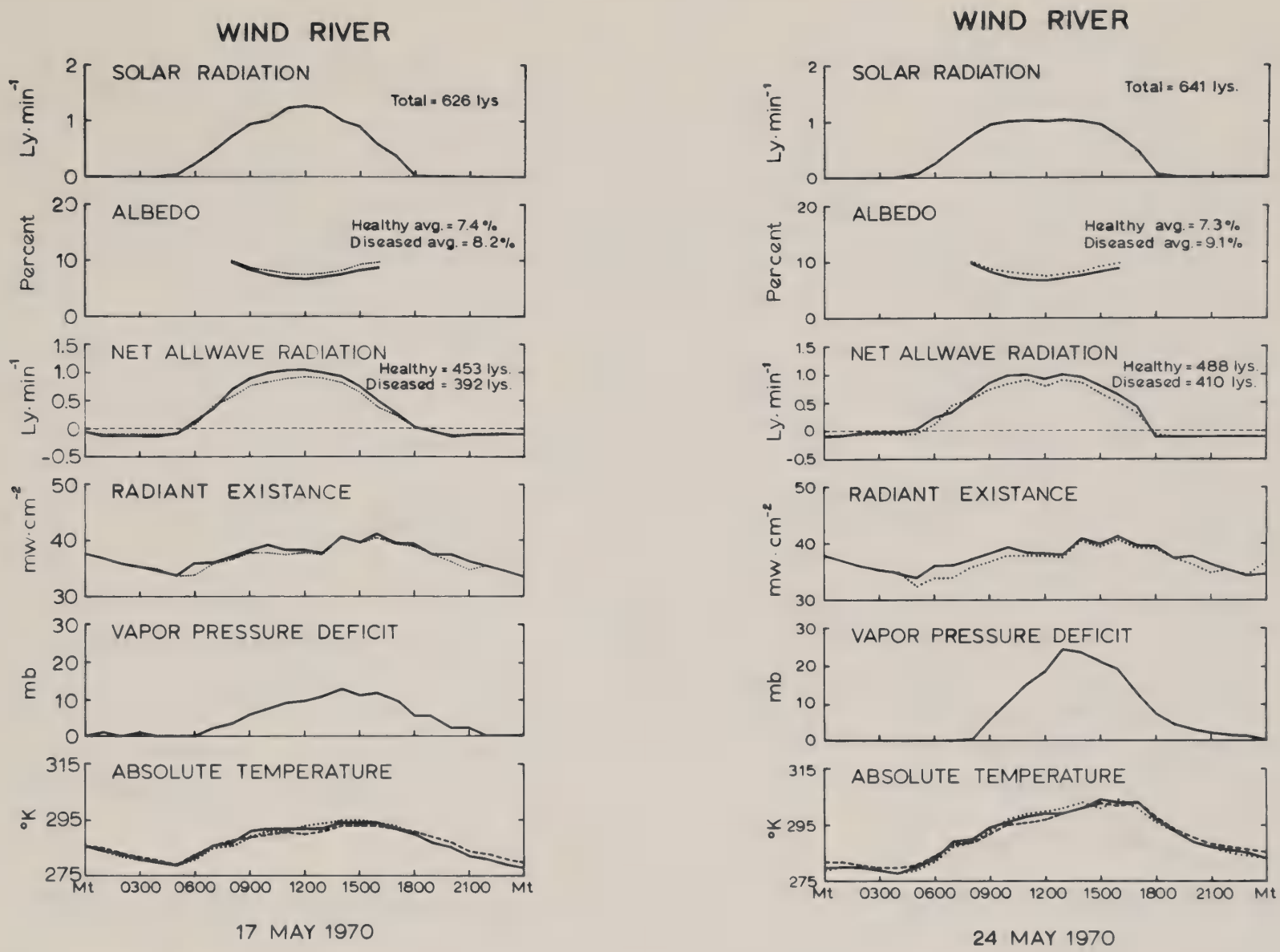

Figure 8. Differences in biophysical response between healthy and Poria-infected Douglas fir trees in Washington on May 17 and May 24, 1970. Solid lines represent measurements over healthy trees, dotted lines represent measurements over diseased trees, and in the bottom graph, the broken line represents ambient air temperature. Toward the end of May soil moisture in the root-occupied horizons was still near field capacity at Wind River.

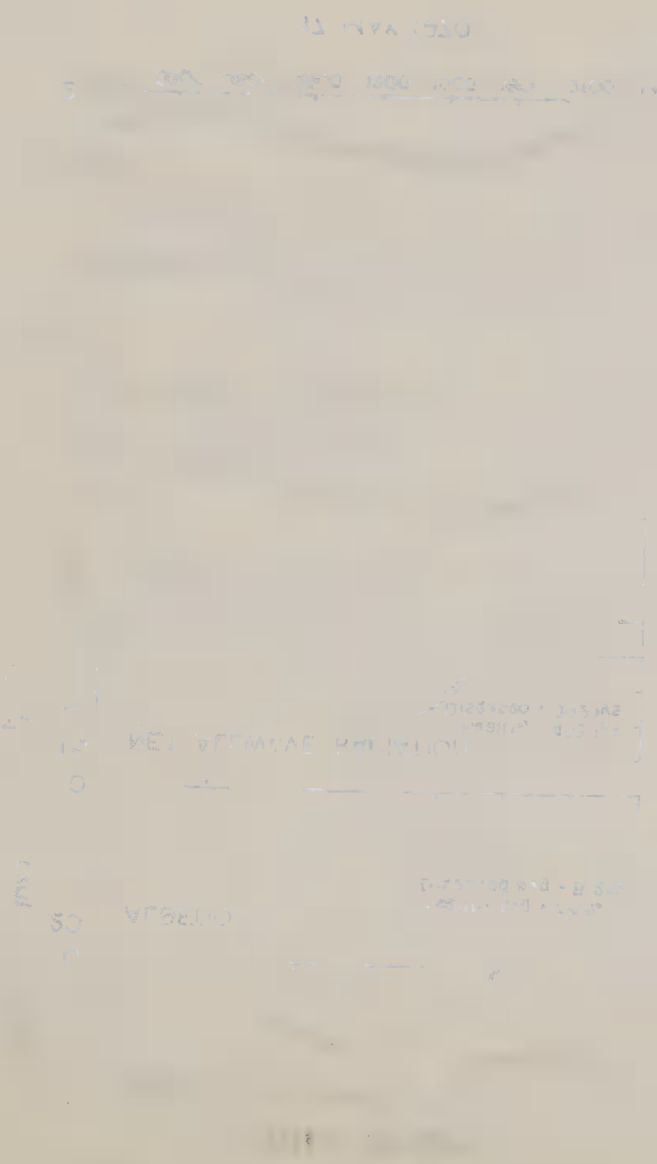

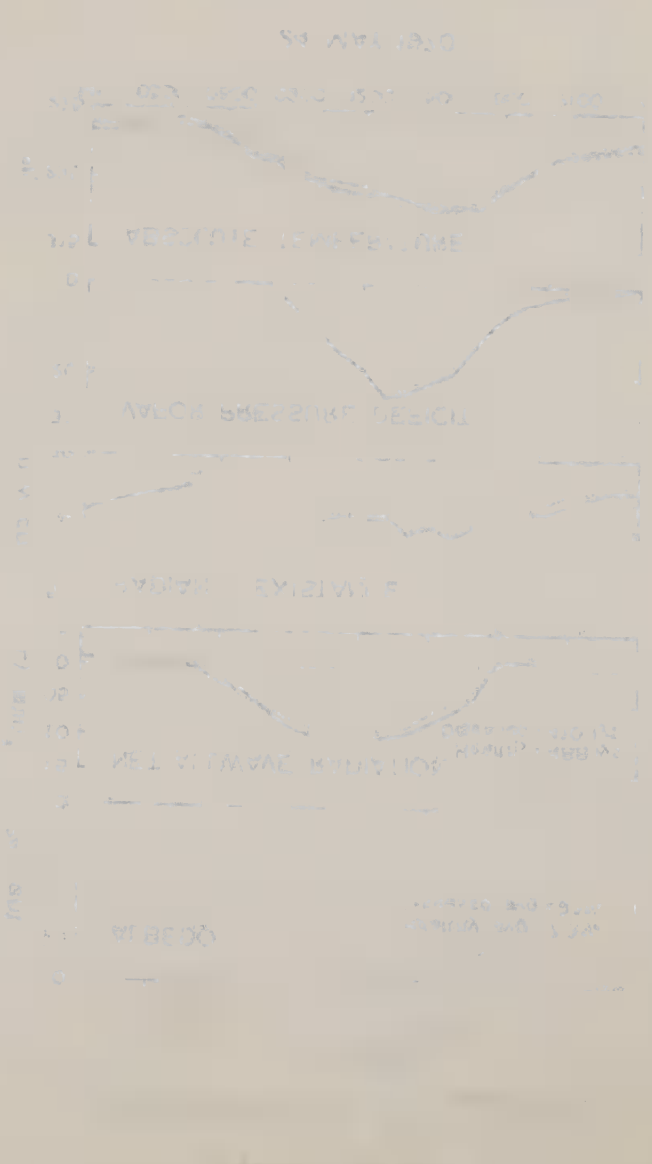

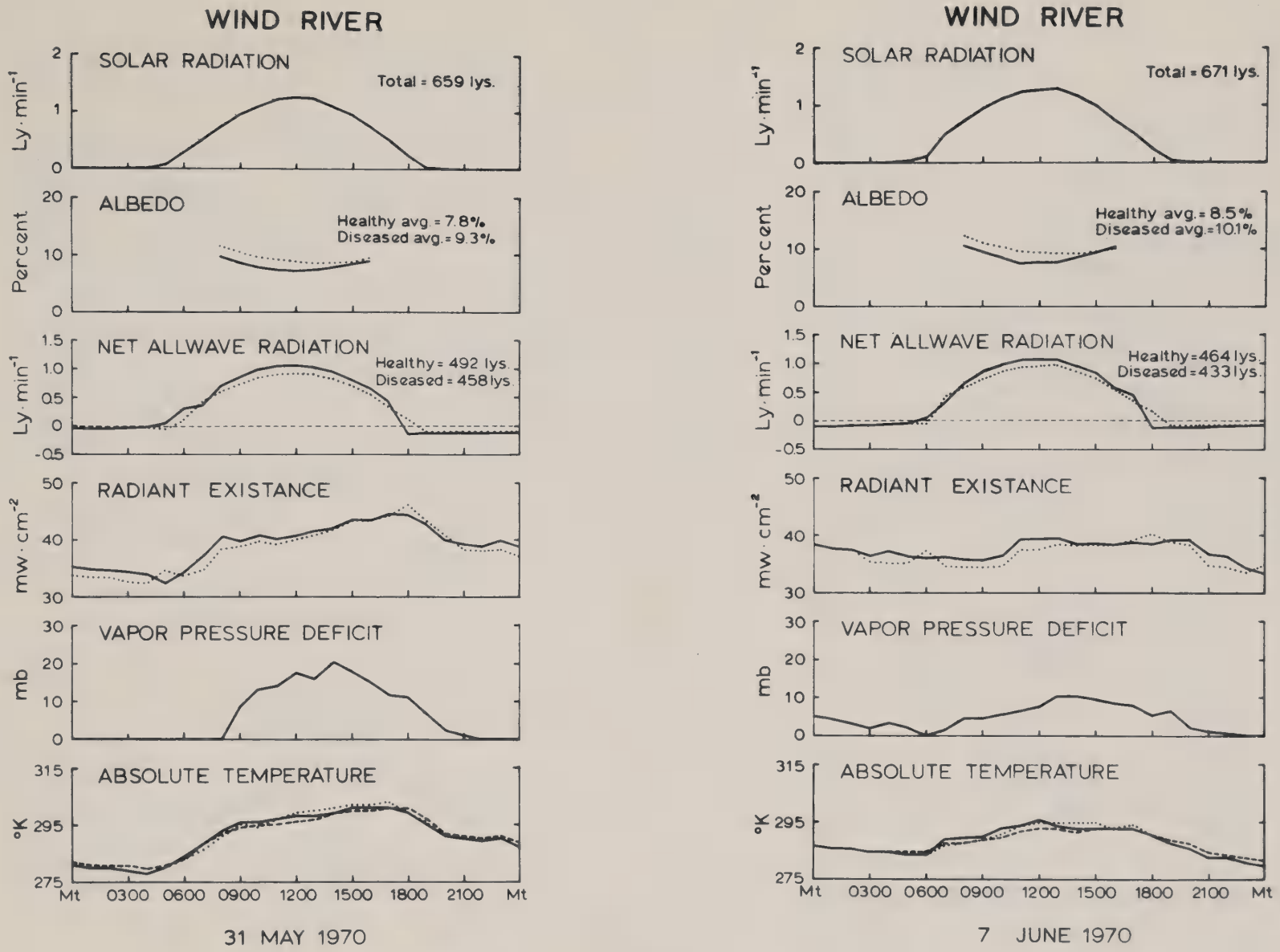

Figure 9. Differences in biophysical response between healthy and Poria-infected Douglas fir trees in Washington on May 31 and June 7, 1970. Solid lines represent measurements over healthy trees, dotted lines represent measurements over diseased trees, and in the bottom graph, the broken line represents ambient air temperature. Midday differences in albedo (shortwave reflectance) are clearly shown between healthy and root-rot infected trees.

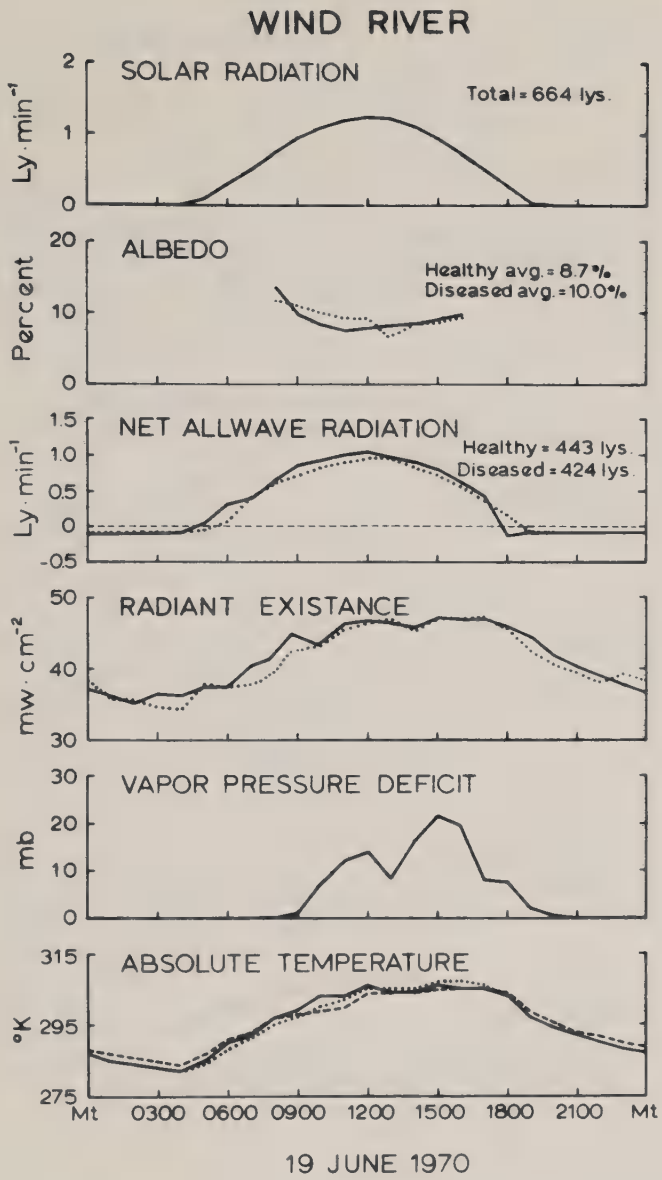

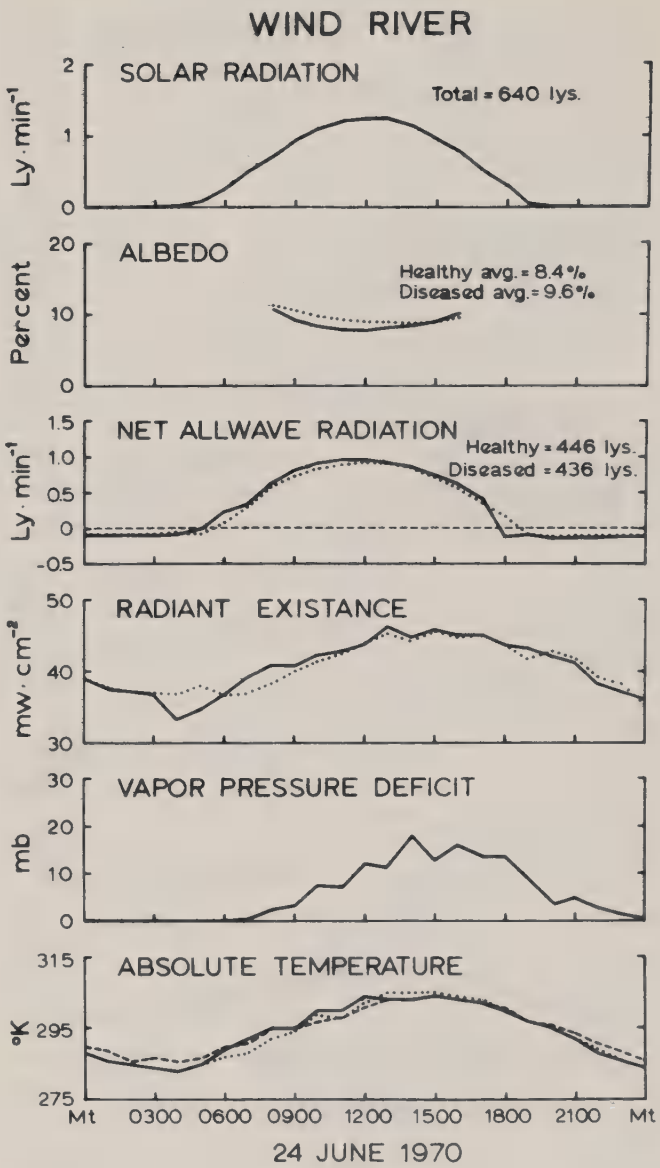

Figure 10. Differences in biophysical response between healthy and Poria-infected Douglas fir trees in Washington on June 19 and June 24, 1970. Solid lines represent measurements over healthy trees, dotted lines represent measurements over diseased trees, and in the bottom graph, the broken line represents ambient air temperature. Soil moisture in the root occupied horizons was still adequate and did not complicate the interpretation of biophysical data with a water stress factor for healthy trees.

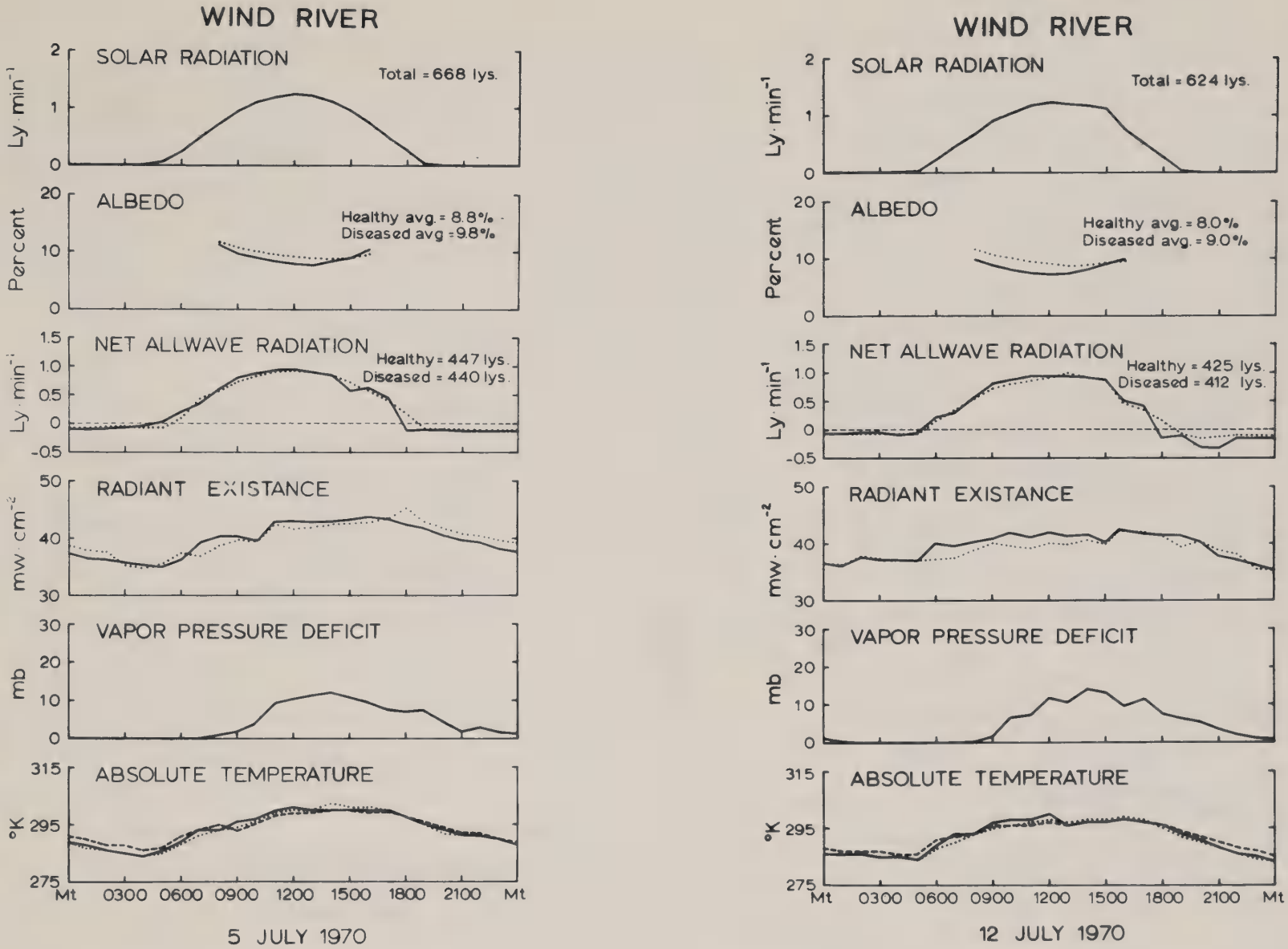

Figure 11. Differences in biophysical response between healthy and Poria-infected Douglas fir trees in Washington on July 5 and July 12, 1970. Solid lines represent measurements over healthy trees, dotted lines represent measurements over diseased trees, and in the bottom graph, the broken line represents ambient air temperature. An interesting phenomenon on July 12, which was not uncommon throughout the summer, was that while midday albedo continued higher for infected trees, radiant existance of healthy trees was actually higher than for root-rot infected trees.

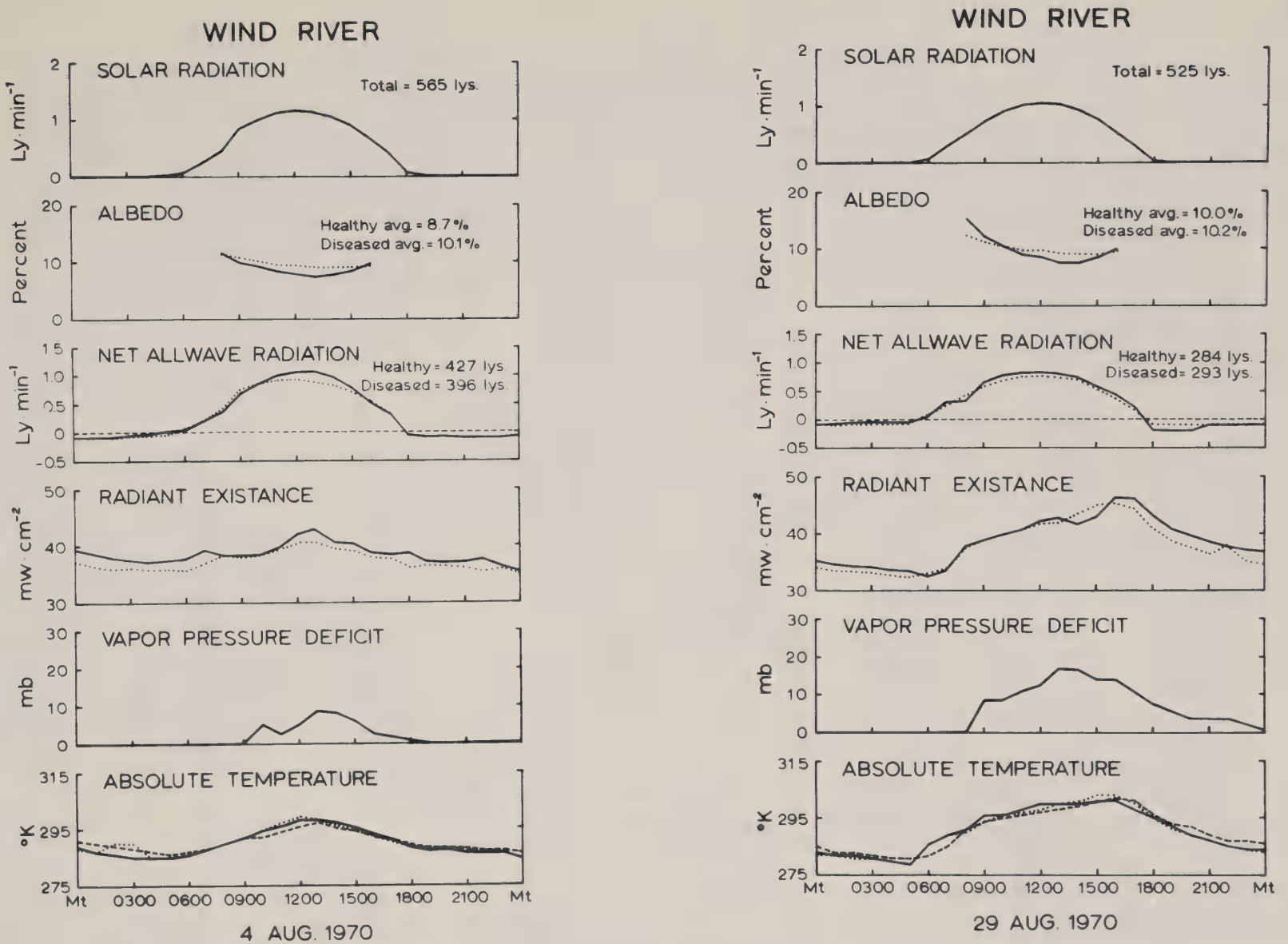

Figure 12. Differences in biophysical response between healthy and Poria-infected Douglas fir trees in Washington on August 4 and August 29, 1970. Solid lines represent measurements over healthy trees, dotted lines represent measurements over diseased trees, and in the bottom graph, the broken line represents ambient air temperature. The period of greatest soil moisture stress at Wind River occurred during the last week in August. Even then, moisture tension in the root-occupied horizons was far below the wilting point level which, if reached frequently, confuses the interpretation of physiological stress data.

Radiant exitance is a measure of radiant flux of an object such as a tree (Nicodemus, 1970).[1] It is not a measure of radiance, a factor which we had no practical method of obtaining. Radiant exitance is a direct measure of the longwave (thermal infrared) emission of a tree. It is the measure of apparent temperature (3 - 15 μm) and is the same quantity measured by an airborne thermal detector. Our radiant exitance sensors were calibrated to be sensitive to .2°C changes in the temperature of a black body emission source.

Vapor pressure deficit is not an energy value; rather, it expresses a potential for an exchange of energy. It is correlated with potential evaporation; and, we have shown in the past that healthy conifers have a higher calculated potential evaporation factor. This finding was based on a steeper water vapor diffusion gradient between the substomatal cavity and the atmosphere outside the leaf diffusion shell. The implication for remote sensing is that the greatest potential thermal energy differential between healthy and stressed trees occurs during periods of high vapor pressure deficit when healthy trees have a high evapotranspiration rate.

Absolute temperature is a term applied not so much because it is registered in degrees Kelvin but because it is a true measure of the subsurface temperature of the Douglas fir foliage. Depending on the accuracy of the measurement technique, absolute temperatures can provide a convincing measure of temperature differences among trees of different vigor classes. We feel that absolute temperature is a valid measure particularly when taken in concert with radiant exitance data. Our data (Figures 8 - 12) do not differ from established experimental evidence (Gates, 1965) that leaf temperatures

---

[1] We accept the recommendations of Nicodemus for new international nomenclature and symbols for radimetric quantities. We now use radiant exitance for the old term "radiant emittance."

of fir are closely aligned with ambient air temperature. We should now view the energy balance results from Wind River with the perspective of the foregoing discussion.

The three most striking features of the Wind River energy data (Figures 8 - 12) were (1) the high daily total solar radiation input represented by clear days; (2) each sample day shows a higher average albedo, or shortwave reflectance, for Poria weirii infected trees than for healthy trees (the greatest measured differences always occurred at midday); and (3) during the daylight hours, net radiation was lower over diseased trees than healthy trees. Day by day, the magnitude and flux of the net radiation differential (between healthy and diseased trees) closely paralleled the albedo variations. The peculiar shape of the net radiation curves between 1700 and 1900 hours resulted from the sun dipping below the high terrain to the west of the study area.

We looked very closely at the results of radiant exitance data because such data provide the essence of thermal infrared information. Except for a few anomalies, radiant exitance data consistently expressed a higher thermal emission state for healthy trees than for diseased. It is emphasized that the magnitude of the differences was small in terms of an actual temperature difference. However, the higher energy emission state in the healthy trees leads us to believe that the real impact of Poria root rot on the Douglas fir is a small reduction in physiologic processes--principally, respiration and metabolism. This, together with the changed shortwave reflectance, indicates a subtle reduction in vigor.

There were times when radiant exitance was slightly higher for diseased trees. However, as in the case of results on July 5 (Figure 11), the difference occurred at night. We are inclined to view this as an anomaly,

not so much because it occurred at night as because there was no consistency to the pattern for several days running. Daytime patterns of radiant exitance differences usually recurred several days in a row.

Radiant exitance on August 29, 1970 (Figure 12) was higher for diseased trees between 1300 and 1500 hours. This may have had more impact on the interpretation of results--coming late in the summer, when soil moisture deficits are expected--if it had been confirmed by a similar pattern for several days running. Such was not the case, so this, too, cannot be considered relevant.

There were good examples (Figures 8 and 9) of days when vapor pressure deficit (at its peak) potentially could create a large thermal difference between healthy and water-stressed trees. This was at a time when soil moisture was readily available to all trees. Yet on these days when the greatest vapor pressure deficit occurred, the radiant exitance for healthy and diseased trees was nearly equal. This, more than any fact, leads us to believe that Poria weirii at Wind River imposes a low-grade stress on infected trees which is maintained over a long period of time. The impact causes very subtle changes in external physical features over time which results in differences in shortwave reflectance. However, it does not appear to cause any drastic change in physiology during the day or throughout the summer which would be useful to detection by thermal remote sensing.

The Pol-tek acoustical sensor was tested at Wind River on several healthy and diseased trees to determine the presence or absence of Poria weirii root rot. Increment borings were made to verify the amount of rotted wood or incipient fungal staining. In addition, one tree which showed advanced decay was felled and cut into 18-inch sections for inspection. Prior sonic readings were taken at these intervals before the actual condition of

the cross section was observed. Several standing dead trees (snags with no branches) were also checked at the base, two feet, and five feet above the ground.

Although the checking was limited to relatively few trees it was apparent that the acoustical sensor correctly identified rotted or punky material in the cross sections, whether in green standing trees or dead standing trees. Actual meter readings varied with tree diameter. The decrease in readings was clearly evident when the sensor probed rotted wood. The sound wood close to the rotted portions was generally discolored by infection; however, the area of staining did not provide a different reading than solid unstained wood.

Photographic Evaluation

The purpose of obtaining aerial photography was twofold: (1) to provide interpreter orientation on the multispectral imagery for each flight over the research area, and (2) to check for visible indicators--within the sensitivity range of the film and filters used--of incipient root rot infection. The visible symptoms we looked for were discoloration of foliage and foreshortened branch growth.

Photography for all four flights (in July) was acceptable in terms of exposure and coverage except for one roll of color film that was lost due to a malfunction of one 70 mm. camera. This created no problem in the evaluation. However, loss of color balance and resolution in the film duplication process that produced the working film copies we received left much to be desired. Although there was little information loss in duplication of the panchromatic and aerographic infrared film, we felt considerable information was lost in the poor quality color and color infrared film copies.

We were able to use all the film for (1) locating study trees, (2) locating the towers and tramways, and (3) identifying forest type and tree species. Because of the similarity of coverage between the photographic and the scanner data, we used the panchromatic photography (exposed through a red filter) for point location on the scanner imagery.

After intensive examination of all the photography, we concluded that there were no instances of "seeing" incipient root rot damage from Poria weirii, either from color differences or from other external physical symptoms. The only stress factors identified were several groups of old growth Douglas fir killed by the Douglas fir beetle. However, the dead trees were fully discolored (red-yellow foliage) at the time of the flights.

Multispectral Evaluation

Multispectral video data were examined for each flight. In general, all the raw data was good, although some was better because the aircraft traversed the preplanned flight line more precisely.

A large number of analog and digital processing techniques were tested because of the flexibility allowed by having the raw data registered and referenced. Those techniques reported here were the most applicable to our detection problem. Results are presented in order for the following analyses: (1) likelihood ratio on SPARC, (2) Euclidean distance on SPARC, (3) thermal slicing, and (4) thermal digital.

Likelihood ratio processing of three-channel infrared data (1.0 - 1.4 μm, 2.0 - 2.6 μm, and 4.5 - 5.5 μm) on SPARC seemed in the beginning to hold the most promise for identification of Poria-infected fir. The three registered channels included an extension of photographic infrared on channel one, a good foliage water stress detection on channel two, and a thermal infrared

band on channel three.

A seven-target SPARC discrimination model was set into the analog processor which seemed quite accurate and was judged to be a tight model on the basis of accurate recognition within the training areas. The model included identification of (1) alder, (2) healthy fir, (3) infected fir, (4) fir/hardwood subcanopy (background), (5) hardwood/fir subcanopy (background), (6) dry nursery, and (7) wet nursery.

Total area recognition (Figure 13) was accurate for all targets except diseased fir. The color-coded mosaic of likelihood ratio processing showed that the only infected fir identified was inside the two-tree training area. All the other ground checked Poria trees were identified as healthy. We hasten to add that this is exactly the way they appear to most ground observers.

After processing several runs of the best three-channel infrared data with the same results we concluded that: (1) likelihood ratio processing on SPARC will produce a very accurate forest type map in a Douglas fir community but (2) will not identify incipient Poria weirii root rot infection centers.

Ten-channel spectrometer data, .4 - 1.0 μm, were processed by SPARC using Euclidean distance analysis. A four-target recognition model was set up on the processor using six of the ten data channels which contributed the most to spectral discrimination. They were (1) .4 - .44 μm, (2).55 - .58 μm, (3) .58 - .62 μm, (4) .62 - .66 μm, (5) .66 - .72 μm, and (6) .8 - 1.0 μm. The training sets were (1) healthy fir, (2) infected fir, (3) alder, and (4) nursery.

The six-channel discrimination model provided a realistic recognition map (Figure 14), depending on the threshold voltage selected. That is, healthy fir, alder and nursery were clearly recognized, but again, as in the

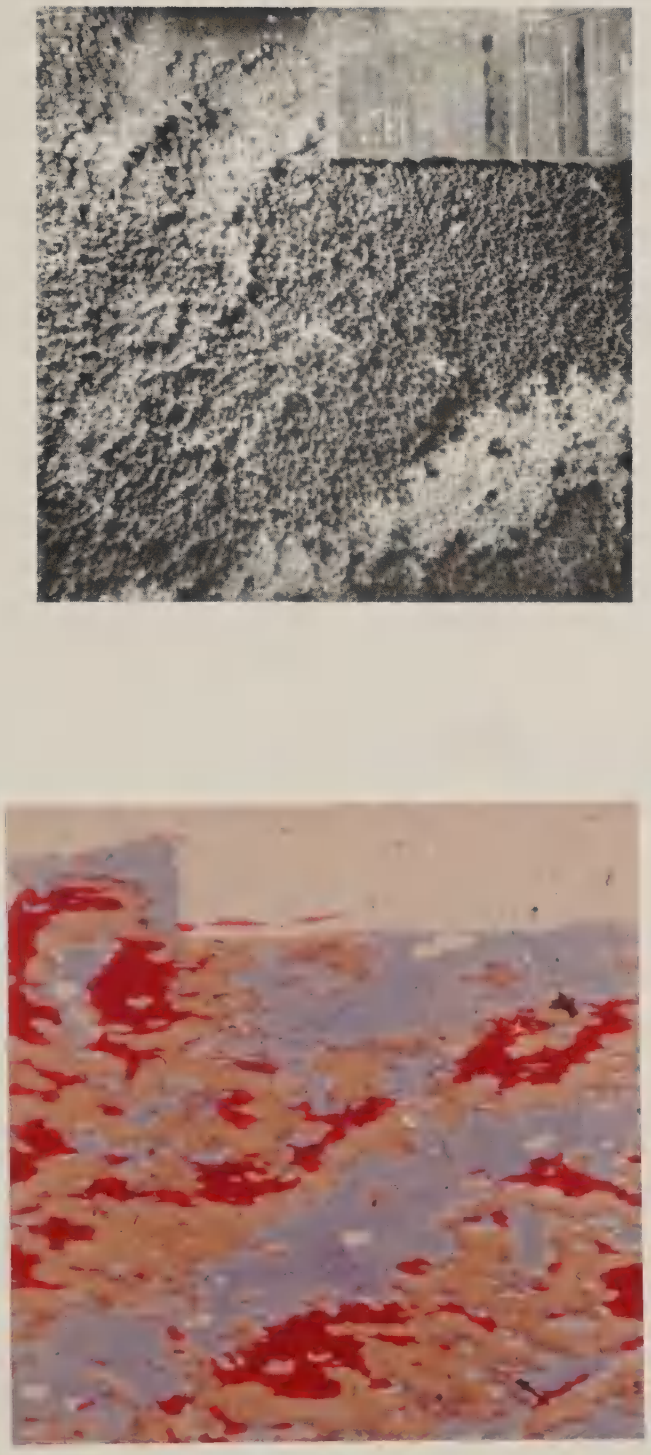

Figure 13. Aerial photo (top) gives perspective for interpretation of color mosaic (bottom) which resulted from likelihood ratio processing of three-channel infrared data (1.0 - 1.4 μm, 2.0 - 2.6 μm, and 4.5 - 5.5 μm) on SPARC. On the mosaic, healthy fir is green, infected fir is sepia (only the diseased training model shows), alder is amber, wet nursery is blue, and dry nursery is brown.

Figure 14. Aerial photo (top) gives perspective for interpretation of color mosaic (bottom) which resulted from Euclidean distance processing of ten-channel spectrometer data on SPARC. On the mosaic, healthy fir is amber, diseased fir is red (only the training model shows), and alder is blue.

case of the three-channel model, Poria-infected fir was only recognized inside the training set. All other infected firs were incorrectly identified as healthy fir. We surmise that the effects of the low-grade stress previously discussed resulted in fewer and shorter needles in the infected trees. The effect was to expose more bark area, as viewed from above, which increased blue reflectance. However, if this is true, the condition, no matter how subtle, would be best revealed on an ultraviolet (.32 - .38 μm) detector.

Thermal infrared data (8 - 14 μm) were examined in detail and the best run from each of the four flight periods was selected for both analog and digital processing. Results of single-channel analog thermal processing are shown (Figure 15). These results were the most sensitive attained by thermal slicing techniques at the Willow Run Laboratories and represent a color-coded difference of 0.5°C between the colors displayed. Actual thermal slices were made at the equivalence of 0.1°C but significant changes were only revealed in every fifth slice. The uniqueness of the thermal display identifies alder trees as warmest and two categories of healthy Douglas fir as cooler. The differences identified within fir were not healthy versus diseased trees, but rather two different stand densities of healthy fir.

The thermal analyses were also displayed digitally as a computer produced greymap with density of the computer printout calibrated to variation in radiant exitance (Figure 16). Radiant exitance of the nursery was often much higher than for the forest, causing the spread of the greymap characterization to include a range of radiance, thereby losing sensitivity over the forest. In order to provide the best thermal sensitivity, the grey scale was often kept within the narrow range of radiant exitance measured over the forest.

Within the four data runs processed, there was no evidence of higher

Figure 15. Aerial photo (top) gives perspective for interpretation of color mosaic (bottom) which resulted from thermal slicing of 8 - 14 μm thermal infrared data. Uniform thermal radiance characteristic of a Douglas fir forest is illustrated by the fact that warmest to the coldest slice, which represents the total scene, are only 4° C apart at midday.

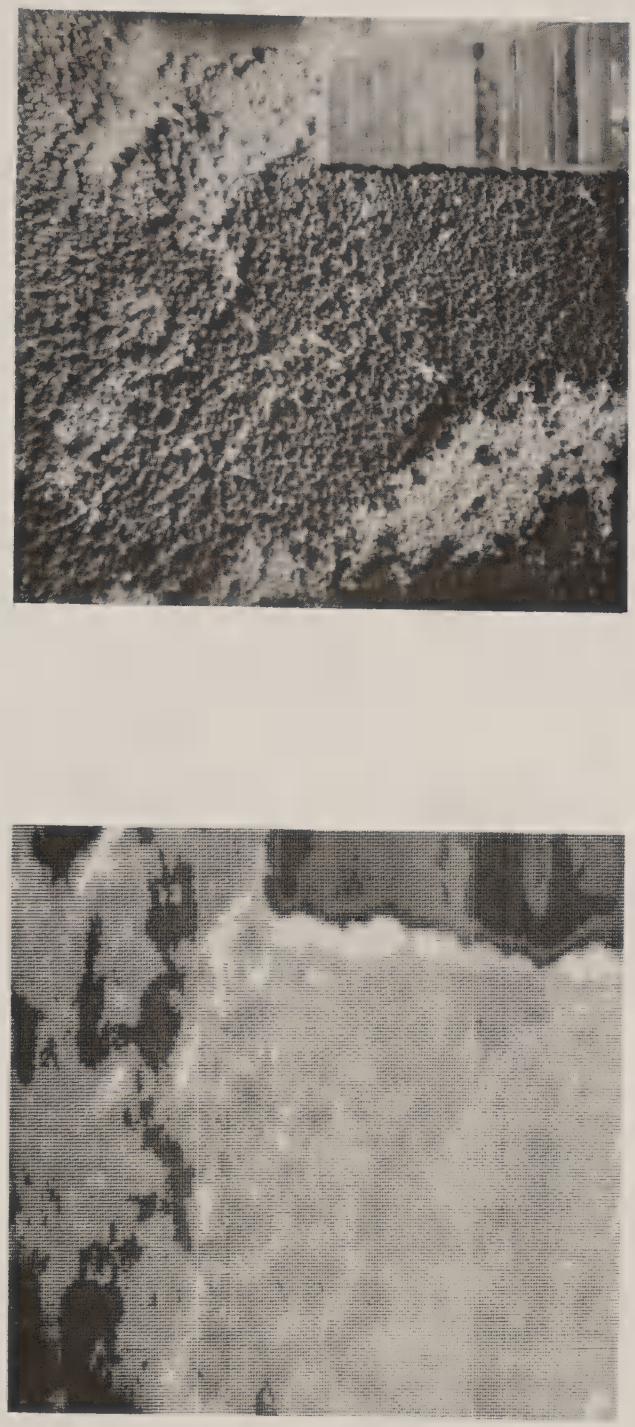

Figure 16. Aerial panchromatic photograph (top) exposed through a Wratten 25A (red) filter at a scale of 1:8,000 on a midday flight July 14, 1969 over the Wind River research area. On the same flight the University of Michigan's multispectral aircraft recorded data for thermal greymap (bottom). Greymap was produced by special single-channel digital processing of 8 - 14 μm infrared data which was analyzed on a 1604 computer at the Willow Run Laboratories.

radiant exitance over the Poria-infected study trees in spite of refined digitizing and sampling techniques which allowed about 15 (thermal) samples for each tree crown. To reduce the size of the output format, the computer output usually printed every fourth data sample on the greymap. Although this was somewhat laborious, we could go directly to the location of each study tree on the greymap, using an enlargement of the original thermal analog.

After summarizing the great volume of processing results we concluded that incipient infection of Poria weirii to Douglas-fir stands cannot be identified solely by SPARC processing of airborne spectrometer data (.4 - 1.0 μm) or three-channel infrared data (1.0 - 5.5 μm). Further, thermal infrared sensing (4 - 14 μm) holds little or no promise for identifying Poria-infected trees. This important fact was verified by extensive ground studies and sophisticated processing (both analog and digital) of airborne multispectral data.

SUMMARY

Remote Sensing Rationale

The focus of our research over the past two years has been to identify stress factors in Douglas fir infected with Poria weirii root rot, and to relate the importance of those factors--if any--as input to a remote sensing system. This focus was suggested by results of apparent temperature measurements made during the summers of 1967 and 1968 which indicated infected trees had higher apparent temperatures during the daytime (Wear, 1967 and 1968).

Research on bark beetle and fungus-attacked pine trees had pinpointed water balance and energy profile factors which influenced airborne identification of stress trees (Weber, 1969). More directly, it was determined that

SUMMARY

Remote Sensing Applicable

a reflectance and emittance signature remotely recorded is a direct expression of tree (physiological) vigor. Water movement to the tree crown and the resulting leaf water potential played an important role in the assessment of tree vigor from the air. That is, attacked trees which suffered impairment of normal upward water translocation had much lower leaf water potentials and higher radiant exitance.

Our preliminary data from Wind River prior to 1970 indicated that perhaps Poria weirii infection manifested the same type of energy profile change. We felt that if it were established scientifically that root rot infection caused a disruption to internal water balance in Douglas fir, then there would be a sound basis for "seeing" an expression of stress from the air.

Biophysical and Physiological Implications

We found little in the thermal data to suggest that there might be thermal radiance differences between tree condition classes at the Wind River research area. In fact, from intensive analysis of 120 continuous days of data, only isolated examples of thermal differences were found between healthy and infected trees. Those anomalous cases could not be related to any physiological or environmental phenomenon, although the latter is more likely to be true. We strongly believe that, as a general case, radiant exitance differences between healthy and stressed trees are brought about through differential water availability and metabolism in the upper crown of large trees. In the case of Poria weirii, we could not measure consistent patterns of water use as a function of apparent tree condition.

One important implication to remote sensing was derived from shortwave radiation data; that is, the two percent higher albedo at midday which was

consistently recorded over infected trees as compared to healthy trees. Together with our other energy data this finding suggests that if a difference is ever to be detected for incipient infection centers by remote sensors, it will be between .32 and 2.6 μm.

Multispectral Imagery

The application of airborne multispectral remote sensing and the potential of automatic multispectral processing for detection of incipient root rot damage to Douglas fir were investigated. Optical-mechanical line scanners and an array of aerial reconnaissance cameras were flown by the University of Michigan's Willow Run Laboratories over our highly instrumented research site at Wind River. The overflights resulted in our obtaining excellent quality multispectral imagery in 18 discrete channels between 0.4 and 13.5 μm.

Advanced methods of multispectral image processing, both analog and digital, were used at the Willow Run Laboratories in an attempt to identify a uniqueness of Poria weirii infected trees. Multiple-channel processing of registered data was done in two areas (.4 - 1.0 μm and 1.0 - 5.5 μm) and specialized single-channel processing was used for thermal infrared data, 8 - 14 μm.

We were not successful in identifying incipient root rot infection in Douglas fir, which had been our goal. We did determine, however, that the combination of optical-mechanical scanner data and automatic processing techniques would produce a very accurate forest species type map in a Douglas fir community. Also, we inadvertently located several Douglas fir bark beetle infestation spots which happened to be on our flight line. The attacked trees were discolored with red-yellow foliage at the time of the over-

flight and were easily identified on several of the spectrometer bands.

Although it is doubtful that remote sensors will locate individual or groups of fir trees with *incipient* root rot infection in the near future, it is possible that an extended range spectrometer with registered data between .32 and 2.6 μm may detect *advanced* stages of *Poria* infection. This is especially likely if the infection center is relatively large and associated with holes in the forest canopy.

Future Research

A new dimension in identifying spectral signature indicators for *Poria weirii* root rot disease in Douglas fir evolved with the discovery of large infection centers on panchromatic photography (Figure 17). The photo recognition feature is the unusually shaped openings in the forest canopy first noticed on the 1:15,840 scale photography of the Oregon high Cascades. Without *a priori* knowledge it could not be determined which of several possible phenomena caused the openings. They may have resulted from insect or disease disturbance, unusual geomorphological features such as rock outcrops or otherwise sterile soil, or perhaps from a combination of special soil and water conditions that caused a discontinuity in the forest type.

Preliminary examination of three areas by a team of forest biologists revealed that *Poria weirii* was prevalent and had killed Douglas fir and hemlock trees. Other trees in the general area (western white pine, red cedar, white fir, and mountain hemlock) were found to be unaffected by the root rot disease. The irregular bare strips and openings were between 20 and 40 feet wide and formed a pattern 100 to 300 feet long. It is apparent that the ringworm-like circular patterns resulted from the spread of the disease. The openings were found to result from fallen and largely disintegrated

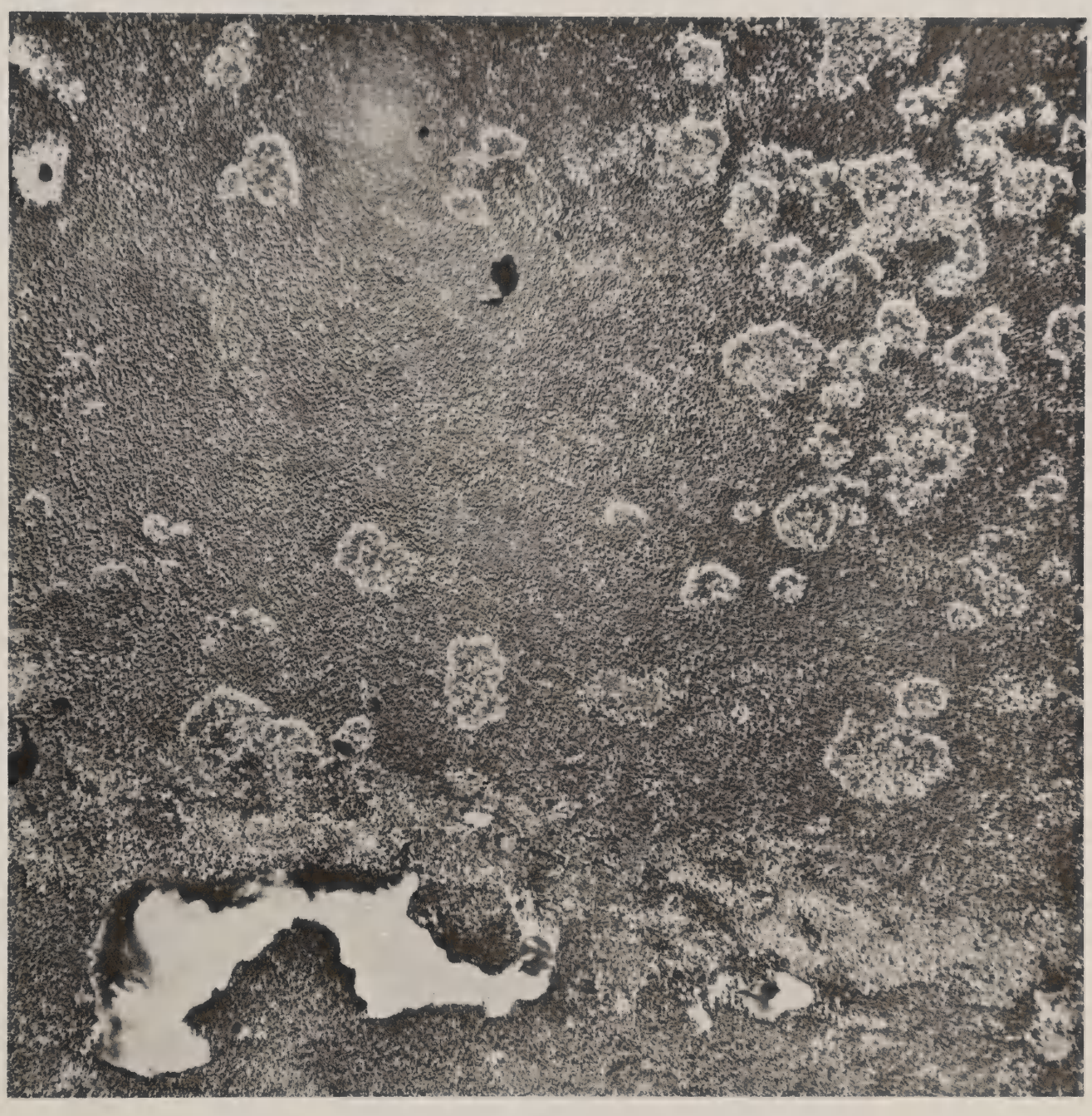

Figure 17. Centers of large Poria weirii root rot infection have been identified on 1:15,840 scale panchromatic aerial photographs like the one shown, which is near Waldo Lake in the Oregon high Cascades. The "ringworm" appearance of the spreading infection was verified on the ground as caused by dead root rot-infected trees.

tree trunks.

It is our intent to focus future research on this promising signature indicator of *Poria weirii* root rot.

LITERATURE CITED

Gates, D. M. 1966. Heat transfer in plants. Sci. Am., 213 (6).

Lowe, D. S., J. G. N. Brathwaite & V. L. Lorrowe. 1966. An investigative study of a spectrum-matching imaging system. Final Report 8201-1-F, Willow Run Laboratores, Institute of Science and Technology, University of Michigan, Ann Arbor, Michigan.

Nalepka, R. F. 1970. Investigation of multispectral discrimination techniques. Report No. 2264-12-F, Willow Run Laboratories, Institute of Science and Technology, University of Michigan, Ann Arbor, Michigan.

Nicodemus, F. E. 1970. Reflectance nomenclature and directional reflectance and emissivity. Appl. Optics 9 (6).

Wear, J. F. 1967. The development of spectro-signature indicators of root disease on large forest areas. Sci. & Tech. Aerosp. Reps., NASA.

_____. 1968. The development of spectro-signature indicators of root disease on large forest areas. Sci. & Tech. Aerosp. Reps., NASA.

Weber, F. P. 1969. Remote sensing implications of water deficit and energy relationships for Ponderosa pine attacked by bark beetles and associated disease organisms. Doctoral dissertation, University of Michigan, Ann Arbor, Michigan.

APPENDIX

The following is a list of USDA Forest Service personnel who have made contributions to this research study and represent a major salary contribution to it.

Pacific Southwest Forest and Range Experiment Station, Berkeley:

Harry W. Camp, Assistant Director

Margaret Dugan, Secretary to the Assistant Director

Joyce Dye, Computer Programmer

Robert C. Heller, Project Leader

Richard J. Myhre, Forestry Research Technician

Mary Twito, Forestry Aide

James Von Mosch, Forestry Technician

John F. Wear, Forester

Anne Weber, Project Clerk

F. P. Weber, Research Forester

Marilyn Wilkes, Mathematician

Pacific Northwest Regional Office, Portland:

Ben Howard, Branch Chief

Jim Stewart, Pathologist

Jack Thompson, Pathologist

Pacific Northwest Forest and Range Experiment Station, Portland:

Wally C. Guy, Photographer

R0001 018739

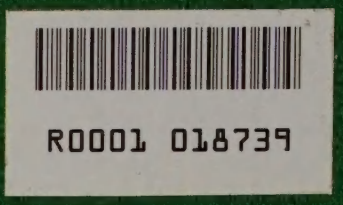
R0001 018739